X-linked muscular dystrophy in a Labrador Retriever strain: phenotypic and molecular characterization.

Barthélémy Inès
Institut Mondor de recherche biomedicale https://orcid.org/0000-0002-4747-5893
Inès Barthelemy
Institut Mondor de recherche biomedicale
Nadège Calmels
Hopitaux universitaires de Strasbourg
Robert B. Weiss
University of Utah Department of Human Genetics
Laurent Tiret
Institut Mondor de recherche biomedicale
Adeline Vulin
Universite de Versailles Saint-Quentin-en-Yvelines
Nicolas Wein
Nationwide Children's Hospital
Cécile Peccate
Institut de Myologie
Carole Drougard
Institut Mondor de recherche biomedicale
Christophe Beroud
Hopital de la Timone
Nathalie Deburgrave
Hopital Cochin
Jean-Laurent Thibaud
Institut Mondor de recherche biomedicale
Catherine Escriou
VetAgro Sup
Isabel Punzon
Institut Mondor de recherche biomedicale
Luis Garcia
Universite de Versailles Saint-Quentin en Yvelines UFR des Sciences
Jean-Claude Kaplan
Hopital Cochin
Kevin M. Flanigan

Nationwide Children's Hospital

France Leturcq

Hopital Cochin

Stéphane Blot (stephane.blot@vet-alfort.fr)

https://orcid.org/0000-0002-8982-0317

Research

Keywords: Dog, canine, Neuromuscular disorders, animal model, DMD, LRMD, Dystrophin, Inversion, Dp71

Posted Date: March 6th, 2020

DOI: https://doi.org/10.21203/rs.3.rs-16251/v1

Version of Record: A version of this preprint was published on August 7th, 2020. See the published version at https://doi.org/10.1186/s13395-020-00239-0.

Abstract

Background Canine models of Duchenne muscular dystrophy (DMD) are valuable to evaluate therapies because they faithfully reproduce the human disease. Several cases of dystrophinopathies have been described in canines, but the GRMD (Golden Retriever Muscular Dystrophy) model remains the one used in most preclinical studies.

Methods We report a new spontaneous dystrophinopathy in a Labrador retriever strain, named LRMD (Labrador Retriever Muscular Dystrophy), for which a colony was established. Fourteen LRMD dogs were followed-up and compared to the GRMD standard.

Results The clinical features of the GRMD disease were found in LRMD dogs, and the functional tests provided data roughly overlapping those measured in GRMD dogs, with similar inter-individual heterogeneity. Molecular techniques including RNA-sequencing allowed to map and identify the LRMD causal mutation, consisting in a 2.2-Mb inversion disrupting the DMD gene within its intron 20, and involving TMEM47 gene. In skeletal muscles, the Dp71 isoform was ectopically expressed as a probable consequence of the mutation. We found no evidence of polymorphism in the two LTBP4 and Jagged1 modifier genes that would explain the observed inter-individual variability.

Conclusions This study provides a full comparative description of a new spontaneous canine dystrophinopathy, that we demonstrate is phenotypically equivalent to the GRMD model. We report a novel large DNA mutation within the DMD gene and provide evidence that LRMD is a relevant model to pinpoint additional DMD modifier genes.

Background

Duchenne muscular dystrophy is an X-linked inherited disorder due to mutations in the Dystrophin gene, which large size explains the relatively high incidence of this genetic disease affecting 1 in 3600 to 9300 male births [1]. The dystrophin-deficiency leads to severe muscle lesions including necrosis, regeneration, inflammation, fibrosis and fatty degeneration. The patients initially present with gait difficulties and frequent falls and are usually diagnosed around five years of age [2]. The disease is then rapidly progressive and leads to a permanent use of the wheelchair at around 10 years of age. During teenage and young adulthood, respiratory muscle weakness progresses, patients need ventilatory assistance, and a dilated cardiomyopathy develops [2]. Both respiratory and cardiac insufficiencies lead to premature death of these patients in their third to fourth decade, despite the dramatic progress in the medical management of these patients made over the last decades [2, 3].

In parallel to this active clinical research that has substantially increased the lifespan but also the quality of life of the DMD patients, innovative therapies including gene, cell and pharmacological therapies have been and are developed with the aim to cure or alleviate DMD. The phase of development of such strategies requires validation steps in animal models. Among the animal models of DMD, dystrophin deficient dogs reproduce the main histopathological and clinical features of DMD, in a large size

organism [4, 5]. Therefore they represent a challenging preclinical context, compared to smaller animals, to ultimately validate the functional benefit provided by large-scale produced therapeutic agents, and secure the translation to humans [5–7].

Twenty-nine spontaneous muscular dystrophy cases have been described in 26 different dog breeds, belonging to 9 over the 10 canine breed groups [5, 8–34]. Causative mutations in the dystrophin gene have been identified in 14 dog strains: a Cocker Spaniel with a 4 bp deletion in exon 65 [5], a Corgi with an insertion in intron 13 [22], a Cavalier King Charles Spaniel with a splice site mutation in intron 50 [23], another Cavalier King Charles Spaniel with a 7 bp deletion in exon 42 [30], a Rottweiler with a non-sense mutation in exon 58 [14], a Tibetan terrier with an exon 8 to 29 deletion [5], a German shorthaired pointer and a miniature Poodle with a large deletion of the whole DMD locus [16, 31, 35], a Norfolk terrier with a 1 bp deletion in exon 22 [27], a Japanese Spitz with an inversion in the intron 19 [29], a Border Collie with a 1 bp deletion in exon 20 [32], a Labradoodle with a point mutation in exon 21 [33], a Labrador retriever with a 184 bp insertion in intron 19 [5], and a Golden retriever with a splice site mutation in intron 6 [36]. The latter mutation was maintained in the Golden retriever background, or introgressed into the Beagle background [37], both models having been extensively used in preclinical trials for DMD.

The so-called GRMD (Golden Retriever Muscular Dystrophy) dog is well known and described: clinical signs include early and progressive gait impairment, dyspnea, dysphagia and delayed dilated cardiomyopathy, altogether resembling the human DMD clinical profile, including a strong inter-individual heterogeneity, under investigation to identify disease modulators [4, 38–40]. Quantitative evaluation tools, often adapted from techniques used in patients, have been developed for the GRMD dog model, and have allowed demonstrating promising beneficial effects of therapies for DMD at the preclinical step [41–44]. However this model is sometimes criticized because of the inter-individual heterogeneity, in addition to its low availability [6, 45]. The GRMD mutation located out of the DMD major hotspot of mutations, is therefore not a perfectly similar genetic context to most of DMD cases [23], and the presence of revertant fibers might be confusing by conferring an immune tolerance to engineered dystrophins [7]. Therefore the interest of candidate canine models, alternative or complementary to GRMD should be investigated each time a spontaneous case is identified. Recently, the intron 50 mutation identified in Cavalier King Charles, introgressed and maintained in a beagle background, has been used to provide proof of concept of successful targeted gene editing in DMD dogs [46].

Here we report a canine X-linked muscular dystrophy in a Labrador retriever strain, named LRMD (Labrador Retriever Muscular Dystrophy), for which a breeding colony was established. In this paper, we provide a comprehensive molecular and clinical characterization as well as a functional description, relative to the reference GRMD dog model, in order to evaluate the possible interest of this model in genetic or preclinical studies.

Methods

Animals and colony establishment

The two first affected dogs (LRMD1 and 2) belonged to a Labrador retriever breeder, and were referred at the age of 4 months by their veterinarian to the neurology consultation of the Alfort school of veterinary medicine (EnvA), where they underwent complete neurological assessment, CK dosage, electromyographic studies, and muscle biopsies. The breeder donated to the Neurobiology laboratory (EnvA) two affected brothers from another litter (LRMD3 and 4) as well as a sister with a 50% risk to be a carrier. A first litter, obtained from this female and the male LRMD4, contained an affected male and an affected female attesting the heterozygous status of the dam. A colony was then established from these two founders and using crossings between affected males and carrier females. The reproduction was assisted by artificial insemination. A total of 10 litters allowed the obtention of 26 LRMD dogs among which 10 remained alive after 1 month of age. A total of 14 LRMD dogs were thus studied (4 born in the breeding farm and 10 in the laboratory) among which 9 males and 5 females. Before having the genetic diagnosis available, the LRMD dogs' identification was based on sustained high serum CK values, and on clinical and histological observations; the unaffected females were de facto considered as heterozygous due to the crossing which was used (diseased father). For ethical reasons, the breeding of this colony has now been stopped and frozen semen from LRMD males has been saved in order to be able to rebuild a colony if needed.

Survival analysis

A first Kaplan-Meier survival curve was performed encompassing all the born LRMD (n = 30). Given the fact that the GRMD dogs are not bred in the laboratory but in an external breeding farm to arrive in the lab around two months of age, the comparison of the survival between both colonies was performed from the age of two months. The 14 LRMD dogs having survived after two months of age were compared with 181 GRMD dogs that were not included in any systemic treatment protocol, and to 14 healthy dogs from the GRMD colony. Survival data were censored in two cases: if a dog was still alive at time of the analysis, or if the dog left the laboratory to be adopted, in the case of healthy dogs. Percentiles of survival were calculated in the software Statistica 10 (StatSoft ®). A Kaplan-Meier curve was also obtained and a log-rank test used to compare GRMD and LRMD survival.

Clinical scoring

The dogs were clinically scored using the grid developed and validated in the laboratory for GRMD dogs [47]. Seven LRMD dogs (three females, four males) underwent iterative clinical scoring from weaning (2 months of age) and during their whole life. Their clinical scores were compared to values obtained in an age-matched male GRMD population encompassing 21 animals, using t-tests, and the dispersion of both populations was evaluated by calculating coefficients of variation. Seven LRMD dogs (three females, four males) including five among the seven longitudinally followed-up animals underwent clinical scoring at an adult age (mean 23.6 months, SD 12.0 months, min 13.9 max 46.4 months). Eleven adult male GRMD dogs (mean 23.2 months, SD 13.9, min 9.9 max 49.3 months) were used to compare both colonies using a t-test, given that there was no significant difference in ages of both populations ($p = 0.9$).

Gait analysis using 3D-accelerometry

The gait quality was quantified using a method previously described in GRMD dogs based on 3D-accelerometric recordings near to the centre of gravity during spontaneous locomotion [48]. Briefly, the dogs were prompted to walk or run along a corridor, and were allowed to self-select their gait and speed. During the test, 3 orthogonally-positioned accelerometers inserted in a small device (Locometrix ®) were maintained near to the xiphoid process using a thoracic belt, and recorded accelerometric curves (acquisition frequency 100 Hz).

A dedicated software (Equimetrix ®) was used to calculate the following variables, described as relevant in growing GRMD dogs: the speed, the stride frequency, the stride length, the regularity, the dorso-ventral, cranio-caudal and medio-lateral powers, and the total power. The speed and stride length were used after normalization by the height at withers, and the axial powers were expressed as relative powers after a normalization by the total power.

Three LRMD dogs (two female, one male) could be tested iteratively during the progressive phase of the disease. The first test was performed between 2 and 3 months of age, and the dogs were subsequently tested every two weeks until the age of 9 months. They were compared to a population of 24 age-matched male GRMD dogs and 6 healthy male golden retrievers. Four LRMD dogs (2 females, 2 males) were tested at an adult age (mean 20.7 months SD 10.4 months, min 12.7 months max 35.4 months) and compared to 18 male GRMD and 11 healthy male adult golden retriever dogs (mean GRMD 17.8 months SD 14.5 months ; mean healthy dogs 21.3 months, SD 21.9 months). As previously described [49], a principal component analysis (PCA) using 7 variables (the stride frequency, stride length, regularity, the three relative powers and the total power), the 18 GRMD and the 11 healthy dogs as active individuals was performed in order to produce a reference PCA plane that represents 90.6% of the variance (68.2% by the component 1 and 22.4% by the component 2). In order to position the LRMD dogs relative to GRMD and healthy dogs, they were projected as supplementary individuals on this PCA plane.

Force measurement

An in vivo force measurement on both hindlimbs was performed at the age of 4 and 6 months in two LRMD dogs (one male, one female), as previously described [50]. The dogs were generally anaesthetized using a propofol (6.5 mg/kg) intravenous induction, and a maintenance with isoflurane in 100% O_2. A continuous monitoring of ECG, SpO2, ETCO2, rectal temperature was set up, and an automatic ventilator was used to maintain normocapnia. They were positioned in dorsal recumbency and their both hindlimbs were successively positioned into a dedicated device already used to assess muscle force after therapeutic procedures [42, 51]. The device was composed of two force transducers (HBM PW6DC3) linked to a vertical plate supporting the anatomical segment encompassing the tarsus, metatarsus and digits. The tarsus was 90° flexed, so that the leg rested horizontally, the femur being vertically positioned by gently maintaining a 90° flexion of the knee. A percutaneous stimulation of the fibular nerve was performed, and the stimulation intensity progressively increased until force reached a plateau, and then increased by 150% in order to ensure supramaximal stimulation. Once the supramaximal stimulation intensity was fixed, 6 1-minute-spaced tetanic stimulations (50 Hz, 2 seconds duration) were applied, leading to the contraction of the cranial compartment of the leg inducing a tarsal flexion and a digital

extension. The signal produced by the transducers was amplified (Grass CP122 amplifiers), and digitally converted and recorded (iWorx 214 and Labscribe software). The maximal tetanic isometric force was obtained by averaging the values of the six tetanic contractions. For the analysis, and to compare animals with different sizes (healthy dogs larger than diseased ones), this absolute force value was normalized by the length of the leg measured in the force measurement device, leading to a relative force index (N/m). Since an incomplete relaxation after a tetanic contraction is seen in GRMD dogs [50], this type of abnormality was also looked for in LRMD dogs. The post-tetanic residual contraction index was calculated as the difference between the baselines before and after the tetanic contraction, and expressed as a percentage of the tetanic absolute force. The results obtained in the two LRMD dogs were compared to age-matched values obtained in 8 healthy and 17 GRMD age-matched dogs, examined at 4 and 6 months of age. Given the low number of tested LRMD dogs this comparison remained qualitative (no statistical test performed).

Respiratory function analysis

Two different methods already routinely used in GRMD dogs by us and others were used to evaluate the respiratory function of LRMD dogs [52]. The first one is based on fluoroscopic acquisitions focused on the diaphragmatic region, performed using a fluoroscopy imaging system (GE® OEC 9800). Conscious dogs were positioned in right lateral recumbency, reassured and gently maintained in this position during a 9 second acquisition at 25 Hz that could be repeated in case of low respiratory frequency, in order to record a minimum of four respiratory cycles. End-inspiratory and end-expiratory images were used to calculate the range of motion of the diaphragm: the ventral edge of the caudal vena cava foramen was tagged in both images, which were then superimposed in order to measure the distance between both tags, in the software Photoshop CS3. This diaphragm excursion distance was normalized by the length of the 13th thoracic vertebra on the images in order to take into account differences in dogs' size. A second indice was calculated on end-expiratory images, to quantify the position of the diaphragm at rest. The angle formed at the ventral edge of the diaphragmatic foramen of the caudal vena cava, by a perpendicular to the vertebral axis and a straight line joining the caudal edge of the 11th thoracic vertebra was measured, in the software Visilog 7.0. The lowest the angle is, the more caudally retracted is the diaphragm. Four adult LRMD dogs (two males and two females) were tested at a mean age of 24.0 months (SD 17.1 months; min 9.0 months; max 44.9 months), and compared with five adult healthy male dogs (mean 15.2 months of age SD 5.3 months min 10.7 months max 23.8 months) and eleven adult GRMD male dogs (mean 25.0 months, SD 24.3 months; min 9.7 max 77.5 months).

The second method used was the analysis of Tidal breathing flow-volume loops, acquired on conscious dogs. A pneumotachometer (Spirobank II, MIR®) was linked to a tight-fitting facemask placed over the muzzle including lip commissures. Tidal breathing flow-volume loops were acquired and analysed in the software WinSpiro PRO (MIR®). A selection of loops without any artifact was performed and the following measurements were used: the peak expiratory flow (PEF) and the peak inspiratory flow (PIF) defined as the maximal flow value registered during the expiratory/inspiratory phases, and the expiratory flow once 75% of the expiratory volume is reached (EF75). Two ratios known of interest in GRMD dogs

were then calculated: the PIF/PEF and the EF75/PEF ratios [52]. Four adult LRMD dogs (two males and two females) were tested at a mean age of 24.9 months (SD 16.0 months; min 9.9 months; max 44.7 months), and compared with eight adult healthy male dogs (mean 23.1 months of age SD 8.1 months min 11.0 months max 37.5 months) and eleven adult GRMD male dogs (mean 25.7 months, SD 25.0 months; min 9.6 max 77.9 months).

Comparisons between LRMD and healthy or GRMD dogs were performed using t-tests.

Echocardiography

Two LRMD dogs could be examined using echocardiography: LRMD4 at 5 months of age, and LRMD7 at 5.4 and 7.4 years of age. Dogs were unsedated during the imaging session. Conventional 2D and M mode echocardiography was performed. In particular, a right parasternal short axis view 2D-guided M-mode acquisition allowed the calculation of the shortening fraction (%). In complement, in the youngest dog, tissue doppler imaging was performed and the difference between systolic left free-ventricular endocardial and epicardial velocities was calculated and named myocardial gradient of velocities, as previously described [53].

Histological techniques

Muscle biopsies were either surgically taken, with the same anaesthetic protocol as for the muscle force measurement with a morphine-ensured per-operative analgesia, or were sampled during necropsy. They were immediately vertically mounted on a cork-piece, using tragacanth gum, and snap-frozen in isopentane cooled in liquid nitrogen. They were kept at -80 °C before cutting. Biopsies were cut at -28 °C using a cryostat (CM3050S, Leica). Sections of 10 µm were used for morphological stainings, and sections of 7 µm for immunohistological experiments.

Histopathological evaluation using H&E staining

Dried sections were stained 10 minutes in hematein and 5 minutes in 1% Eosin, dehydrated in four consecutive baths of ethanol, and mounted in Canada balsam after a soak in xylene. A total of 112 biopsies from different skeletal muscles of diseased dogs until the age of 76 months were sampled and qualitatively evaluated. Among these biopsies, 38 were taken at necropsy from neonates. Still among these 112 samples, a selection of 33 biopsies from different skeletal muscles (biceps femoris, sartorius cranialis, tibialis cranialis, vastus lateralis, triceps brachii, extensor carpi radialis and diaphragm), sampled at different ages (2 to 24 months) were analysed using a pathological quantification based on a random sampling and annotation of histological events on entire sections as previously described [50].

Alizarin red S staining

Dried sections were stained during 5 minutes in a 2% alizarin red S solution at pH 5.4. They were rinsed and dehydrated in acetone and acetone-xylene volume/volume, and mounted in Canada balsam. Fibers with a normal calcium content appeared pale pink, whereas the calcium overloaded fibers appeared deep

pink, to bright red for the more strongly overloaded. This staining was used on the 38 biopsies from deceased neonates in order to investigate a potential neonatal form.

Immunohistochemistry

Seven- micrometers sections from each biopsy were dried, rehydrated and fixed in cold acetone-methanol. Antibodies against dystrophin were all used at a 1:20 dilution and were either purchased from Novocastra: NCL-Dys2 (C-terminal part), NCL-Dys 1 (rod domain repeats 8–9), or kindly gifted by Pr Glenn E. Morris (CIND): MANEX1A (N-terminal part of dystrophin), MANEX1011C (rod domain repeat 1), MANDYS107 (rod domain repeat 15). Secondary antibodies used were anti-mouse FITC (1:50) or Cy3 (1:800) (Jackson Immunoresearch laboratories Inc.).

Western blot

Multiplex Western-Blot

Muscle protein analysis, including dystrophin, was performed on muscle surgical biopsy samples by multiplex Western blot analysis using the procedure described by Anderson and Davison [Anderson LVB, Davison K, Am J of Pathology, 1999]. Monoclonal antibodies used for multiplex Western blots are from Novocastra (Newcastle, United Kingdom; www.novocastra.co.uk). For multiplex Western blots combinations of antibodies are as follows: 1) multiplex A includes the antibodies Dys8/6C5 (NCL-DYS2/dystrophin C-ter), Cal3c/2A2 (NCL-CALP-12A2/calpain 3 exon 8), 35DAG/21B5 (NCL-g-SARC/g-sarcoglycan), and Ham1/7B6 (NCL-Hamlet/dysferlin); 2) multiplex B includes the antibodies Dys4/6D3 (NCL-DYS1/dystrophin rod domain), Calp3d/2C4 (NCL-CALP-2C4/calpain 3 exon 1), and ad1/20A6 (NCL-a-SARC/a-sarcoglycan).

Dystrophin Western-Blot

Proteins were extracted from muscle sections using a treatment with 250 mM sucrose, 10 mM Tris pH 7.6, 0.1 mg/ml leupeptin, 1 mg/ml aprotinin, and 20 mg/ml PMSF. After protein dosage (BCA kit, Pierce), the proteins were denatured using a solution containing 20% SDS 20% sol, 20% glycerol, 10% β-mercaptoethanol, and 12.5% migration buffer, and 100 °C heating during 3 minutes. 10% glycerol, and 0.001% bromophenol blue. 250 µg proteins from two muscles biopsies from LRMD3 (biceps femoris, interosseous) were loaded and migrated on a 4–12% NuPAGE Bis-Tris polyacrylamide gel (Life Technologies ®), as well as 50 µg of proteins from a healthy dog’s muscle biopsy. After a transfer on nitrocellulose membrane, the immunoblotting was performed using NCL-Dys2 antibody (Novocastra, 1:50), and secondary horseradish peroxidase-conjugated antibody (1:1000). The membrane was finally revealed using ECL (Amersham).

Identification of the mutation

RT-PCR screening of the Dp427m transcript

Total RNA was extracted from muscle biopsies from LRMD3 and a healthy littermate using the RNeasy kit (Qiagen ®). The reverse transcription was performed using the Superscript II RT kit (Invitrogen®). The Dp427m transcript was explored using nested RT-PCRs with nine pairs of primers designed to amplify overlapping segments of the cDNA, based on the published canine dystrophin cDNA sequence (ESNCAFT00000036277) as follows: exons 3 to 10, exons 10 to 20, exons 15 to 22, exons 21 to 26, exons 25 to 36, exons 35 to 46, exons 45 to 56, exons 55 to 67 and exons 66 to 79 (sequences in Table S1). For these RT-PCR experiments the PCR MasterMix kit (Promega) was used.

Southern Blot analysis

The genomic DNA from two LRMD dogs (LRMD3 and LRMD4) as well as from two unrelated healthy Labrador retriever dogs were studied by Southern blotting after EcoRI restriction. After electrophoresis on 0.8% agarose gel, the DNA was transferred from the gel by passive diffusion to a nitrocellulose membrane. Blots were hybridized with three dystrophin ^{32}P-labeled cDNA probes: probe 1 encompassing exon 18 to 24, probe 2 covering exon 21 and probe 3 covering exon 20. After washing, the membrane was exposed on an autoradiography film at -70 °C.

PCR of the intron 20

Genomic DNA was extracted from blood using DNeasy kit (Qiagen). Four pairs of primers named F1-R1 to F4-R4, allowing the amplification of the whole intron 20 in four overlapping segments were designed based on the published canine dystrophin gene sequence (ENSCAFG00000023562). F1 was designed in the exon 20, and R4 in the exon 21 (sequences in Table S1) Supplementary primers (F4i, and R4i) were designed in between F4 and R4 in order to better explore this zone. Sanger sequencing of the PCR products was performed after DNA gel extraction using the QIAquick gel extraction kit (Qiagen).

RNA-seq analysis

Frozen muscle biopsies were homogenized in 20 mM Tris*Cl pH 7.4, 150 mM NaCl, 5 mM $MgCl_2$, 1 mM DTT, and 1% Triton X-100, and total RNA was extracted from using TRIzol® LS reagent (Life Technologies) followed by isopropanol precipitation according to the manufacturer's instruction. Cytoplasmic and mitochondrial rRNA was depleted from ~ 1 microgram of total RNA using tiling oligodeoxynucleotides and the RNase H digestion method [54]. Illumina TruSeq Stranded Total RNA library kits were used to prepare random-primed, indexed RNA-seq libraries from the rRNA-depleted total RNA preparations and these libraries were sequenced on an Illumina HiSeq 2500 instrument using either single-end 50 bp v4 read chemistry. Quality metrics for FASTQ reads were evaluated with FastQC tool (http://www.bioinformatics.babraham.ac.uk/projects/fastqc) and reads were quality trimmed and adapter clipped using the Trimmomatic tool [55] with standard parameters. FASTQ sequence reads were mapped to the Broad CanFam3.1/canFam3 (Sep. 2011) reference genome using the STAR v2.7 RNA-seq aligner [56]. Strand-specific coverage plots were generated from the alignment files using the BEDTools genomecov function and displayed in the UCSC genome browser after conversion with the UCSC bedGraphToBigWig utility.

Genetic diagnostic test development

In order to be able to reliably identify healthy, carrier and affected animals, a PCR-based genetic test was developed. The F4R4 pair corresponding to the 5' end of the intron 20 was used to amplify the WT allele. A pair of primers across the distant breakpoint, named mutF-mutR (normal size 1939 bp) and supposed to amplify the WT allele but not the LRMD one was also designed. PCR was set up using the Phusion high fidelity DNA polymerase (Thermo Scientific ®). The LRMD F4-mutR and mutF-R4 bands were gel extracted using a Nucleospin Gel and PCR Cleanup kit (Macherey-Nagel), and Sanger sequencing was performed in order to characterize the mutation breakpoints. The diagnostic PCR was designed to be run with three primers in a single PCR: F4, R4 (1661 bp band WT allele), and mutR (890 bp band LRMD allele).

RT-PCR of the Dp71 transcript

Total RNA was extracted from tissues using the RNeasy kit (Qiagen ®). The following samples were used: liver from a healthy dog (Dp71 expression positive control), biceps femoris muscle from a healthy dog, a GRMD dog and a LRMD dog (LRMD8), sartorius cranialis, tibialis cranialis muscles from a LRMD dog (LRMD8). The reverse transcription was performed using the Superscript II RT kit (Invitrogen®). cDNA concentration was determined by spectrophotometry (Nanodrop). The PCR was performed on 120 ng of each of the 7 cDNA samples using the Phusion high fidelity DNA polymerase (Thermo Scientific ®). The forward primer was designed at the junction of the specific first exon of the Dp71 transcript and the exon 63 of the Dp427 transcript (exon 2 of the Dp71), the reverse primer was designed at the junction between exons 64 and 65 of the Dp427 transcript (exons 3–4 of the Dp71) based on published canine sequences AY566609 and ENSCAFT00000036277 (Sequences in Table S1). The expected size of the PCR product was 164 bp.

Jagged1 PCR and sequencing

A PCR involving the point G > T mutation described to lead to very mild clinical forms in GRMD dogs was run in 5 LRMD dogs with diverse phenotypes, using the primers published in [39] and the Phusion high fidelity DNA polymerase (Thermo Scientific ®). Sanger sequencing of the PCR products was then performed in order to look at this point mutation in the promoter region of the Jagged1 gene.

LTBP4 SNPs analysis

The Ensembl genome browser was used to identify known polymorphisms in the 30 coding exons from the canine latent transforming growth factor beta binding protein 4 (LTBP4) gene. Genotypes at these variant sites were called from the RNA-seq data from 5 LRMD dogs (LRMD 8, 9, 10, 12 and 13) using the Genome Analysis Toolkit (GATK, https://software.broadinstitute.org/gatk) best practices workflow for SNP and indel calling on RNA-seq data. The known sites in LTBP4 ENSCAFG00000005133 included 4 missense SNP variants (Ensembl Variant ID: rs851496729:p.Pro425Thr, rs851016279:p.Ser439Pro, rs853156464:p.Pro545Ala, and rs21954920:pAla668Thr) and 7 synonymous SNP variants (Ensembl

Variant ID: rs851354589, rs21999801, rs21954918, rs853084197, rs851625070, rs852260326, and rs850783330); no novel coding variants were observed from the LRMD RNA-seq data.

For all the statistical tests performed, the level of significance was set at $p \leq 0.05$.

Results

First cases report

Two four-month-old male Labrador retriever littermates owned by a breeder were referred by their veterinarian to the neurology consultation of the Alfort school of veterinary medicine. The puppies presented with gait stiffness, exercise intolerance, and marked palmigradic and plantigradic posture (Fig. 1A). At the clinical examination, normoreflexia and absence of proprioceptive defect were observed. The two puppies had markedly elevated serum creatine kinase (LRMD1: 83000 UI/L; LRMD2: 30000 UI/L), and the electromyogram (EMG) revealed normal nerve conduction velocities, but spontaneous activity in all the tested muscles (mainly complex repetitive discharges, Fig. 1B). Muscle biopsies from the biceps femoris muscle were sampled on both dogs and revealed lesions of active necrosis, regeneration, endomysial fribrosis and few inflammatory foci with calcifications (Fig. 1C). The phenotype of these two dogs, together with the high CK, the myopathic EMG profile and the histological lesions were evocative of a muscular dystrophy process. An immunostaining of the biopsies showed no reactivity with an anti-dystrophin antibody directed against the central rod domain (Dys 1, Fig. 1D). A multiplex western blot was also performed (Fig. 1E), confirming the absence of Dp 427 dystrophin, and the presence at expected size of other proteins implicated in human limb-girdle muscular dystrophies: dysferlin, γ-sarcroglycans, and calpain 3. Another litter was obtained by the breeder from the same parents, and once more two affected males were born, reinforcing the hypothesis of an X-linked transmission. The breeder kindly gifted to our research unit these two affected males (LRMD3 and 4) as well as an unaffected daughter from the same parents possibly carrying the causal mutation, allowing us to establish a LRMD colony in the same facilities as a pre-existing GRMD one.

LRMD colony establishment

A first litter was obtained by crossing the presumed female carrier and one of the affected males (LRMD4), and the subsequent litters were obtained by crossings between the descendant dogs (carrier females x affected males). The inbreeding of the colony was high (ranging from 25% for LRMD5 and 6, to 41% for LRMD11 to 14). Over a period of 6 years, ten litters were obtained (Fig. 2). A total of 14 LRMD dogs (9 males and 5 females) survived the neonatal period and were followed-up.

Main phenotypic features

Neonatal period

At birth, the LRMD dogs had a weight comparable to their healthy littermates, but rapidly showed for most of them striking difficulties to suck and needed intensive nursing during their first days to ensure their survival (feeding by oro-gastric gavage, temperature monitoring and stay in incubator if needed). Despite these cares, around 50% of the LRMD newborns died within their 48 first hours (Fig. 3A) following a paroxystic weakness episode associated for most of them by a severe dyspnea. Myoglobinuria could be assessed in some of these puppies, as well as very high serum CK values (> 100000 UI/L) and hyperkalaemia. The rhabdomyololysis was confirmed in these animals, with a selective involvement of some muscles such as the diaphragm, the tongue or the sartorius cranialis (Fig. S1), confirming that this mortinatality syndrome reproduces the neonatal fulminating form well described in the GRMD dog model [57].

Clinical observations

Locomotor signs

After few days of intensive nursing, the surviving LRMD puppies became able to suck by themselves and only exhibited growth retardation in comparison to their healthy littermates. At around the age of 2 months, the LRMD puppies showed a stiff gait and difficulties to jump over an obstacle. In the subsequent months, they became stiffer, and rapidly developed posture abnormalities resembling those seen in GRMD dogs notably marked pelvic verticalization, palmigrady and plantigrady. After six months of age most of the LRMD dogs were unable to run and used a walking gait. However, most of them remained ambulant, except one dog, (LRMD8) who completely lost ambulation at 6 months of age and was therefore euthanized. His littermate (LRMD9) also developed a severely compromised locomotion.

Respiratory and digestive signs

At a young age (2–3 months) the LRMD dogs began to show signs of dyspnea mainly paradoxical thoraco-abdominal movements. In the following months, the dogs developed moderate-exercise induced polypnea, noisy breathing, and in some cases intermittent cyanosis accompanied by an elevated serum bicarbonate concentration. Oro-pharyngeal dysphagia became a major feature of the LRMD from the age of 4 months, with a prominent aggravation in the following months. This severe dysphagia probably explained by the co-occurence of markedly reduced jaw opening, prominent macroglossia, retraction of the tongue, and weakness of the paryngeal muscles themselves, was observed in all the LRMD dogs, and was a cause for humane euthanasia for half of them, who were even unable to maintain a convenient hydration state. As a complication of this oro-pharyngeal dysphagia, LRMD dogs frequently developed aspiration bronchopneumonias, which could be successfully treated for most of them, but which caused the death of 4 out of the 14 affected dogs. On chest radiographs, the usual abnormalities found in GRMD dogs were seen: hiatal hernias, megaoesophagus, pectus excavatum, pulmonary hyperinflation associated with a diaphragm flattening [58].

Survival

The mean survival of these 14 LRMD dogs was 21.6 months, with a first quartile at 10.8 months and a third quartile at 31.4 months. The LRMD dog with the longest survival (LRMD7) died at the age of 103.5 months (8.6 years), probably following paroxystic cardiac arrhythmias (sudden death without significant findings at necropsy in a dog known to have prominent ventricular arrhythmias). A compared survival analysis was performed between LRMD and GRMD dogs and showed that LRMD dogs tended to have a better survival (log-rank test $p = 0.01$) despite close curve profiles between both colonies, and very distinct from the one of healthy dogs (Fig. 3B).

Histological observations

Among the studied biopsies, the general trend for a given muscle was a predominance of necrosis-regeneration lesions in dogs younger than 1 year-old. Inflammatory foci and calcifications were observed in some biopsies from 4- and 6-month-old dogs. Later on, the predominant lesions became the endomysial fibrosis and adiposis after two years (Fig. S2). In parallel, the CK values were highly fluctuating but remained roughly strongly elevated during the first year, and decreased to lower values in older LRMD dogs. Among the sampled muscles, the more affected were the diaphragm and the extensor carpi radialis, according to a pathological scoring (pathological index > 60%).

Functional evaluation and comparison with the GRMD model

The overall phenotypic characteristics of the LRMD dogs resemble those observed in GRMD dogs. In order to position the model in comparison to the “reference” GRMD dog model, a quantitative comparative study between both canine muscular dystrophies was performed, using the tools developed to evaluate GRMD dogs.

Clinical score

As a reflect of the disease progression described above, the clinical score rapidly increased during the first months of the studied LRMD dogs, and tended to progress slower or stabilize after 7–8 months. The same type of evolution was seen in the GRMD population (Fig. 4A). However when comparing more in detail both colonies, the LRMD dogs seemed to have a more rapid and homogeneous evolution in the very first months: at the age of 4 months the LRMD dogs had nearly significantly higher scores ($p = 0.07$) and the coefficient of variation of the clinical score was less in the LRMD colony (12% vs 34% in GRMD dogs). After this point, two subpopulations emerged, with two more severely affected LRMD dogs from a locomotor point of view (LRMD8 and 9), suggesting that as in the GRMD colony, there may be a severe form leading to a loss of ambulation in LRMD dogs [38]. The less affected LRMD dogs seemed to have higher clinical scores than GRMD dogs in the 10–16 months interval. This was confirmed by a comparison between both colonies at an adult age (Fig. 4B), showing that LRMD dogs had significantly higher clinical scores (mean 67.5%, SD 12.1%) than GRMD dogs (mean 48.1%, SD 11.7%; $p = 0.005$).

Gait analysis

The LRMD dogs that were gait-tested using accelerometry exhibited similar profiles as GRMD dogs compared to healthy dogs: decreased speed, stride length and frequency, decreased total power and increased medio-lateral relative power signing the waddling gait of these dogs. Among the three LRMD dogs longitudinally followed-up (Fig. 5), two showed values amongst the more affected GRMD dogs, and a decrease of the gait quality with age, notably with a dramatic increase of the gait waddle. The third dog (LRMD14) had rather preserved ambulation, attesting to the existence of an inter-individual heterogeneity in LRMD dogs. Despite this heterogeneity and the low number of animals followed-up, the total power, a very discriminating variable, was found significantly decreased at all tested ages ($p = 0.035$ at 4 months of age, $p = 0.0001$ at 6 months of age, $p = 0.002$ at 9 months of age), similarly to GRMD dogs (no significant difference between both models). The four LRMD dogs examined at an adult age obtained gait indices values overlapping those usually measured in the GRMD population and significantly different from the healthy one ($p = 0.036$ for the stride frequency to $p < 0.0001$ for the total power). No significant difference was found between LRMD and GRMD dogs, though the relative medio-lateral power was nearly significantly increased in LRMD dogs ($p = 0.059$, mean LRMD = 42% (SD = 10%), mean GRMD = 29% (SD = 13%)). When projecting these four dogs as supplementary individuals on a PCA plane constructed using healthy and GRMD adults as active individuals, the LRMD dogs projected in the GRMD cloud, attesting the gait characteristic similarities between both colonies (Fig. 5).

Force measurement

Two dogs could be muscle force-tested, at 4 and 6 months of age. At both ages, the muscle force appeared decreased compared to healthy dogs, at similar level as for GRMD dogs at 4 months of age, and at a more intermediary level at 6 months of age (Fig. 6). Muscle relaxation impairment is a feature of GRMD dogs, with an incomplete relaxation after a tetanic contraction or a twitch, at varying levels in function of the animals, and with a correlation to the severity of the phenotype. This feature was also found in the LRMD dogs, with an increase of this residual post-tetanic contraction at the 6 months of age.

Respiratory function

The four adult LRMD dogs that underwent respiratory tests showed again similar patterns as GRMD dogs. They had a significantly caudally retracted diaphragm as assessed by the angle index ($p < 0.001$), at similar levels as GRMD dogs (no significant difference between both models) (Fig. 7A). The LRMD diaphragm was hypokinetic with a decreased range of motion ($p = 0.005$), but slightly less than GRMD dogs ($p = 0.02$) (Fig. 7B). The flow-volume loops analysis showed the same abnormalities as those described in GRMD dogs including a dramatic flow decrease at the end of expiration, quantified by the EF75/PEF ratio, which was significantly decreased in LRMD dogs ($p = 0.0004$) at similar levels as GRMD dogs (no significant difference between both models) (Fig. 7C). The PIF/PEF ratio was also dramatically decreased ($p < 0.0001$), as in GRMD dogs (no significant difference between both models), however the LRMD dogs tended to overlap with the lowest GRMD values regarding this flows ratio (Fig. 7D).

Echocardiographic findings

The dog examined at a young age (LRMD4, 5 months) exhibited hyperechoic lesions of the left ventricular free wall, but the measures performed using conventional echocardiography were within normal ranges (shortening fraction 47.5%). However the use of tissue Doppler imaging to analyze the radial motion of the left ventricular free wall revealed slightly decreased endo-epicardial gradient of velocity, a hallmark of early presymptomatic dilated cardiomyopathy reported in GRMD dogs [53]. The dog examined at later stages (LRMD7) showed dilated cardiomyopathy with a marked decrease of the shortening fraction evolving with time (21.5% at 5.5 years of age and 10.3% at 7.5 years of age). This dog also showed frequent ventricular arrhythmias (left and right ventricular extrasystoles), which were suspected to have led to the sudden death of this animal one year after the last echocardiographic examination.

Identification of the causal mutation

RT-PCRs covering the dystrophin cDNA led to the amplification of all parts of the DMD transcript in LRMD dogs, with the exception of the sequence encompassing exons 20 and 21. Indeed, RT-PCRs between exons 10 and 20 and between exons 21 and 26 amplified normal products while no product could be obtained between exons 15 and 22 (Fig. 8A).

A Southern blot of the EcoRI-digested genomic DNA of LRMD dogs and using cDNA probes encompassing exons 18–24, exon 21 or exon 20 revealed abnormal bands (Fig. 8B), confirming at the DNA level a putative remodeled spot, mapped between exons 20 and 21 of the DMD gene.

The whole intron 20 (4.5 kb) was then explored using four overlapping couples of primers (Fig. 8C). The three first pairs covered the 3.2 kb 5’ segment of intron 20 and allowed amplification of amplicons at the expected size. By contrast, the fourth PCR using the F4 - R4 primers yielded no amplicon in LRMD dogs (Fig. 8C), pinpointing a sequence remodeling lying in the 1.6 kb of the 3’ region of intron. New primers designed to approach the putative mutation site allowed to correctly amplify the 640 bp segment covering the 3’ end of the intron, and sequencing of the amplicon confirmed a normal acceptor splice in LRMD dogs. However a 700 bp region (X:27,623,229 to X: 27,622,528) was delineated and remained non-amplifiable even using long-range PCR conditions. Altogether, these molecular data confirmed in LRMD dogs a gross genomic DNA rearrangement involving the nearly 3’ end of intron 20. In addition, when compared to a healthy unrelated Labrador retriever, a slight size difference was seen in the amplicon using the F1 – R1 pair of primers, which appeared longer in dogs from the LRMD colony whatever their clinical status (data not shown). Sanger sequencing showed normal donor splice site in LRMD dogs, but revealed the insertion, 960 bp downstream the 5’ extremity of intron 20, of 36 bp including a 21 bp polyA and the repetition of 15 bp of the adjacent normal sequence. This insertion explained the shifted size of the smallest band revealed on the southern blot using the exon 20 probe (Fig. 8B). We identified this insertion in all animals of the colony, including healthy dogs and thus concluded to a DMD-unrelated polymorphism that segregates in this line of Labradors.

The LRMD-causing mutation involving the 3’ region of intron 20 was then approached by RNA-sequencing to measure DMD transcription levels from both exons and introns using strand-specific

libraries prepared from total RNA. This experiment revealed that minus strand transcription from the Dp427m promoter abruptly decreased within the F4 - R4 PCR region between exons 20 and 21 (Fig. 9A). Ectopic transcription was observed in a region normally located 2 Mb farther toward the centromere on the plus strand 100 kb proximal of TMEM47 gene, where this novel transcription continued for ~ 0.3 Mb (X:29,824,000–30,122,000) into a “no man’s land” of the X chromosome. The level and pattern of transcription across this ~ 0.3 Mb region was similar to DMD large introns, suggesting the causal mutation may be a 2.2 Mb inversion disrupting the DMD gene and involving TMEM47 (Fig. 9A).

In light of this characterization, a new PCR experiment was performed intending both to sequence the breakpoint flanking regions, and also to develop a LRMD mutation diagnostic test able to identify carriers, healthy and diseased dogs. A pair of primers (mutF - mutR) was designed flanking the presumed distant breakpoint, and the lack of amplification between them in the LRMD context confirmed the location of a breakpoint between these primers. The use of these primers in combination with primers located flanking the intron 20 breakpoint (F4 – R4) amplified a PCR product in LRMD but not in healthy dogs. The sequencing of these PCR products allowed the precise characterization of the LRMD mutation as a 2.2 Mb inversion of a region encompassing nucleotides 27,622,834 to 29,823,785 and which can be annotated : chrX:g.27,622,834_29,823,788 inv. This inverted region encompassed the entire TMEM47 gene without disrupting it. The sequencing of the two breakpoints revealed a 27,622,834 to 29,823,789 junction on the one hand (PCR F4-MutR), and a 27,622,824 to 29,823,785 junction on the other hand (PCR MutF-R4). This indicated that the inversion is associated with a 9 nt loss in intron 20 and a 3 nt loss in the distant region, probably attesting to the LRMD mutation probably occurred after two double strand breaks 2.2 Mb apart, and repair by non-homologous end joining after inversion of the released fragment. Based on PCR confirmation of the breakpoint from genomic DNA, close inspection of the RNA-seq data revealed several intronic reads that mapped across the 27,622,834 to 29,823,789 breakpoint and several spliced exonic reads that mapped from DMD exon 20 to multiple locations beyond the inversion breakpoint, confirming transcription and splicing from the DMD region. At last, a multiplex PCR was designed to propose a genetic test able to reliably identify LRMD, carrier, and healthy dogs, and confirmed to discriminate the three genotypes (Fig. 9B).

Characterization of the dystrophin expression in muscles

The dystrophin immunostainings performed on LRMD muscle biopsies using an antibody directed against the C-terminal part of the protein (Dys2) showed a faint but undoubted signal with a normal subsarcolemmal localization (Fig. 10A). The amount of Dys2-positive myofibers was evaluated on 32 skeletal muscle biopsies from 7 LRMD dogs at levels ranging from 0.2% (LRMD6, sartorius cranialis muscle) to 44.1% (LRMD1, tibialis cranialis), with a mean of 11.6% (SD = 12.3%). In order to better characterize this protein, monoclonal antibodies cross-reacting with different regions of the protein were used on serial sections. No staining of the Dys2 positive fibers was obtained using any of the antibodies cross-reacting with upstream regions of the dystrophin protein: the staining was negative for the N-terminal part (MANEX 1A), the first repeat of the rod domain (MANEX 1011 C), or for parts of the rod domain located downstream the mutation (Dys1, MANDYS 107 (Fig. S3)) (Fig. 10A). In some rare fibers

however, a positive staining for the N-terminal part of the protein was found (Manex 1A + and Manex1011C+) but these fibers were negative for the C-terminal part (Dys2) (Fig. S3).

A western blot was performed using the Dys2 antibody cross-reacting with the C-terminal part of the dystrophin, in order to know the size of the expressed dystrophin. A band was visible in the two biopsies tested, at around 70 kD (Fig. 10B). Given the cross-reactivity of the protein specifically with an antibody targeting the C-terminal part of the protein, and the size of approximately 70 kD, we addressed the hypothesis of an expression of the Dp71 isoform. A RT-PCR using a forward primer designed in the specific first exon of the Dp71 confirmed an expression of this isoform in the three tested muscle biopsies (Fig. 10C) and was consistent with RNA-seq coverage data observed in the Dp71 region (Fig. 9A). No expression was found in the biopsy originating from a GRMD dog, suggesting that this Dp71 expression is not a compensatory mechanism in a context of canine dystrophinopathy, but rather a specificity of the LRMD context.

Analysis of two modifier genes, Jagged1 and LTBP4

In order to asses if the inter-individual heterogeneity observed in the LRMD colony could be related to polymorphisms in known modifier genes, the mutation in the Jagged1 gene promoter leading to ‘escaper’ phenotypes in dogs [39] was investigated in 5 LRMD dogs with diverse phenotypes, including the mildest and the oldest survivor. The sequence was identical in every tested LRMD dogs. None of these dogs harbored the G > T point mutation described in GRMD escapers.

Further, coding LTBP4 SNPs were analyzed, since polymorphisms in this gene have been described that strongly modulate the mdx mouse and human DMD phenotype [59, 60]. Eleven SNPs were found in the canine LTBP4 coding sequence, among which only 4 were responsible for amino-acid changes (amino acids number 425, 439, 545 and 668). The 5 LRMD dogs tested were all homozygous and identical for each of the SNPs, in particular the 4 leading to amino acid changes: amino acid 425 was a Threonine, 439 and 545 a Proline, and 668 an Alanine. The similar LTBP4 SNPs profile between LRMD dogs shows that this known modifier is, not more than Jagged1, implicated in the inter-individual heterogeneity seen in this dog model. The homozygosity of the tested LRMD dogs relates to the high inbreeding rate of the colony, which probably makes this LRMD model a facilitated context to discover new DMD phenotype modifiers.

Discussion

This study provides a full description of a new alternative canine model of Duchenne muscular dystrophy in a Labrador retriever strain, named LRMD. Since several descriptions of dystrophin-deficiencies have been reported in the canine species (Table S2), the originality of the present study relies in the direct comparison with the ‘reference’ canine model, the GRMD dog. One of the aims of this study was to identify the potential interest of the LRMD model relative to the most commonly used GRMD one. A comparison to other canine models will also be discussed and is summarized in Table S2.

Clinical, histological and functional findings were comparable to what is usually seen in the GRMD model. Interestingly, the evaluation tools developed for the GRMD model were completely transposable to the LRMD, and the values obtained for the most relevant indices used to evaluate GRMD dogs were in most cases perfectly overlapping those obtained. These tools can thus be used in other dog models, and are able to reveal and quantify a dystrophic muscle function profile. For some measured indices, there was a trend towards a slightly more severe phenotype in LRMD dogs. This might be related to the high inbreeding rate of the colony, since it has been reported to be a disease severity enhancer in dogs [5]. The severity of the LRMD disease described here make these LRMD dogs strikingly different, from a phenotypic point of view, from the ones described to be almost asymptomatic, for which the mutation remains unknown [26].

One of the characteristics of the GRMD model, which could argue in favor of the use of an alternative model improving this point, is the strong inter-individual heterogeneity, reported by all the teams working on this model. A special attention was therefore paid to this specific point in the studied LRMD dogs. Despite a very high degree of relationship between studied individuals, which could have accounted for a higher phenotypic homogeneity, an inter-individual heterogeneity, comparable to the one seen in GRMD dogs, was observed in the 14 LRMD dogs followed-up. The only period at which the animals seemed more homogeneous from the one to another was the very beginning of the clinical evolution, i.e. the 2 to 4 months of age period. After that point all the evaluation methods showed a marked divergence between animals, from relatively mildly affected dogs with preserved ambulation, to dogs with severe ambulation disability. These latter may parallel the so-called ‘severe forms’ of GRMD described in the French colony and associated with an early loss of ambulation in around 25% of the dogs [38]. In the present study it was observed in 2 over 14 LRMD dogs suggesting it could be less frequent in this colony, but this should be taken with caution given the low number of LRMD dogs examined. In order to start to look for clues explaining the inter-individual heterogeneity, we focused on two described DMD modifier genes, the first one in dogs (Jagged1) [39] and the second one in DMD patients (LTBP4) [59], but neither of them explained the phenotype variability seen in LRMD dogs. The existence of a wide inter-individual heterogeneity in a context of a relatively homogeneous genetic background (attested by perfect homozygosity in LTBP4 SNPs, and due to the high inbreeding rate associated with the establishment of the colony), makes this LRMD colony a unique opportunity to identify modulators of the disease, in a facilitated genetic context.

The low number of examined dogs is one of the weaknesses of this descriptive study. In particular, for some functional tests, this would probably require the follow-up of supplementary dogs to obtain a complete natural history, in case this model would be used in therapeutic trials. This was due to the concomitancy between the establishment of the LRMD colony and the development of evaluation tools, which explains why the first animals were not evaluated using accelerometry or tidal-breathing flow-volume loops. A limitation was the use of both females and males, which were compared to a purely male GRMD population. The obtention of female LRMD dogs was due to the fact that diseased males were used as fathers, in order to be able to deduce the genotype of females without a genetic testing, since the mutation was not completely characterized when the colony was established. Given the low

number of animals and the fact that all the used indices potentially impacted by the size were normalized to avoid interpretation bias due to size differences, we chose to introduce functional data from female LRMD dogs in this study. However there are some reports stating that female dystrophin-deficient dogs could be less affected than males [4]. In the present case, an inter-individual heterogeneity was seen within the 5 affected females, though the mildest clinical form (LRMD14), and the oldest survivor (LRMD7) were females.

Another optimization axis relative to GRMD dogs for a new canine model would be the mutation type. Most of human DMD cases are due to large mutations and predominantly deletions, preferentially affecting the major hotspot of mutation spanning exons 45 to 55 or to a lesser extent the minor hotspot (exons 2–20) [61]. Duplications also account for a significant part of the identified mutations, with a frequent occurrence of exon 2 duplication [61, 62]. The GRMD mutation is a point mutation in a splice site and therefore not a model of large mutation. Splice site mutations however account for 3% of the DMD referenced mutations. The LRMD mutation is a gross rearrangement, but inversions are a rare cause of human DMD mutations, maybe in part because they are difficult to detect: querying the Leiden Duchenne Muscular Dystrophy database provides 8 inversions entries [63], and 5 supplementary inversion reports have been found in the literature [64–68]. Thus the LRMD mutation, even if located in the minor human hotspot, is not more than the GRMD one a model for most of the human DMD mutations, as it is the case for example of the Cavalier King Charles dog which carries a splice site mutation in intron 50 amenable to exon 51 skipping like 14% of the DMD patients, and recently successfully used in a gene therapy study [23, 46, 61].

The LRMD mutation would not be amenable to exon skipping therapy since it is a too complex rearrangement. However this mutation could serve to modelize complex/large mutations which could not benefit from exon skipping strategies but rather, for example, from gene replacement strategies. In this context the LRMD model can probably be considered as naïve, from an immune point of view, to a portion of the protein spanning exons 21 to 30 (beginning of the Dp260 transcription, presumably preserved). This context is different from the one of the GRMD dog, in which revertant fibers express a protein lacking only exons 3 to 9 or 5 to 12 [69]. Both GRMD and LRMD models are therefore not optimal to modelize immune response questions in the context of most common human mutations. The German shorthaired pointer muscular dystrophy dog (GSHPMD) in which a deletion of the whole dystrophin-gene occurred, as well as the more recently described miniature Poodle are undoubtedly good candidates for such investigations [16, 35]. The GSHPMD deletion not only involves the whole dystrophin gene but also the TMEM47 (Transmembrane protein 47) gene. Though not disrupted in LRMD dogs but only inverted, the transcription of this gene could be perturbed, and this would have to be checked, even if the GHSPMD dog, a canine spontaneous ‘KO’ for this gene, does not exhibit clinical signs more than those due to muscular dystrophy [35]. TMEM47 encodes for a highly conserved transmembrane claudin-like protein, which is implicated in transition from adherents to tight junctions, and is highly expressed in several tissues including the fetal and adult brain [70, 71]. It has therefore been suspected to be implicated in some cases of X-linked mental retardation. Even if a screening involving 16 affected patients revealed no

TMEM47 implication [72], a recent case of TMEM47 disruption has been linked to intellectual disability and language delay [71].

This 15th reported mutation in canine DMD gene was identified using RNA-sEq. This method shows arousing interest in the field of mutation characterization in undiagnosed rare disease and particularly neuromuscular diseases. Even now in the era of Whole Genome Sequencing (WGS) and Whole Exome Sequencing (WES), a significant amount of patients actually still have unknown mutations. RNA-seq has been recently proposed to help detecting mutations in such patients, and reveals particularly powerful in cases of mutations affecting the splicing process, that can escape the WES and WGS [73, 74].

The inversion reported here is the second one causing Duchenne-type muscular dystrophy in dogs, after the resembling mutation described in a Japanese Spitz dogs strain, which disrupts the DMD gene within the intron 19, involves the TMEM47 gene, and disrupts the RPGR (Retinitis pigmentosa GTPase regulator) gene [29]. Interestingly, in this very comparable context, a protein demonstrated to be the Dp71 isoform was also expressed in muscles [29]. This isoform is normally expressed in all non-muscle tissues, and its expression is downregulated during myogenesis. It has been demonstrated that two transcription factors, Sp1 and Sp3 bind to the Dp71 promoter to activate transcription of this short isoform, and that the loss of Dp71 in mature muscle fibers is due to the repression of their expression by MyoD [75], allowing the availability of the sub-sarcolemmal region to the Dp427m isoform. However these examples of spontaneous expression of Dp71 in adult muscle in a context of inversion of the proximal end of the dystrophin gene, unique to our knowledge, also suggest a role for the Dp427m promoter activation on the Dp71 promoter repression. In LRMD and Japanese Spitz cases, the Dp427m promoter could play a regulatory role at distance on the Dp71 transcription, with Dp71 promoter activation maintained because a lack of control from the inverted proximal end of the dystrophin gene. The expression of this isoform composed of the C-terminal part of the Dp427 protein was confirmed to allow the correct localization of members of the dystrophin-associated protein complex. However, the Dp71 lacks actin-binding domains, and has been therefore described as nonfunctional in skeletal muscle, not providing any benefit when expressed in a mdx background, and even suspected to be deleterious [76–78]. This was confirmed by our findings showing similar phenotypes between LRMD and GRMD dogs with a trend towards an increased severity in LRMD dogs, attesting to the lack of functional advantage provided by the Dp71 isoform and maybe confirming a possible deleterious effect. Such an expression of the Dp71 isoform in skeletal muscles has to our knowledge never been described in DMD patients, and represents a discrepancy between this dog model and the human disease. Moreover, it can be questioned if this expression could be counteracted, in this particular model, by a therapeutic fully functional protein, since some competition may exist between both proteins at the sub-sarcolemmal region.

Conclusions

This study provides a comprehensive description of a new canine dystrophinopathy, from the molecular characterization to the quantitative phenotypic description, together with a comparison to the GRMD dog model which is the most commonly used in preclinical trials for DMD. Both diseases were phenotypically

comparable, including inter-individual heterogeneity, and no major advantage of the LRMD model over the GRMD one could be found, for a use in preclinical therapeutic trials. Moreover, the particular mutational and transcriptional context described in the LRMD dog could be confusing in a context of therapeutic trials intending to bring clear responses about DMD treatment options. This model could however be of interest to better understand the mechanisms involved in the dystrophin isoforms transcriptional regulation. Most importantly, the LRMD colony, which displays phenotype heterogeneity in a likely less heterogeneous genetic background than GRMD, represents an opportunity to help identify and validate disease modulator candidates, in a large animal model faithfully reproducing the human DMD disease course.

Abbreviations

DMD
Duchenne muscular dystrophy; GRMD:Golden Retriever muscular dystrophy; LRMD:Labrador Retriever muscular dystrophy; CK:Creatine kinase; (P)EF:Peak expiratory flow; (P)IF:Peak inspiratory flow.

Declarations

Ethics approval

All procedures performed on GRMD dogs were approved by the Ethical Committee of EnvA, ANSES and UPEC under the approval number 20/12/12-18. They were performed in accordance with the relevant guidelines and regulations.

Consent for publication

Not applicable

Availability of data and materials

The datasets used and/or analysed during the current study are available from the corresponding authors on reasonable request.

Competing interests

The authors declare that they have no competing interests

Funding

This work was supported by the Association Française contre les Myopathies (AFM-Telethon, grant nbr 12696), the Ministère de l'Alimentation de l'Agriculture et de la Forêt, and the National Institutes of Health (NINDS NS043264 and NS085238) to KMF, RBW.

Authors' contributions

IB, NC, RBW, LT, AV, NW, CB, ND, JLT, CE, LG, JCK, KMF, FL, SB designed the experiments

SB, KMF and RBW provided fundings

IB, NC, RBW, LT, CP, CD, IP, SB performed the experiments

IB, NC, RBW, LT, AV, NW, CP, CD, IP, SB analyzed the data

IB, NC, RBW, CP, SB wrote the paper

All the authors reviewed and approved the final manuscript.

Acknowledgements

We are very grateful to Pr Glenn E. Morris and the CIND to have kindly provided us with the anti-dystrophin monoclonal antibodies. We thank Dr Robinot for referring the first cases, and the breeder of the first dogs for his kind collaboration. We thank Dr Alain Fontbonne and the whole team of the CERCA (Centre d'étude en reproduction des carnivores d'Alfort) for their precious help to the reproduction management of the LRMD colony and semen cryopreservation. We thank Mireille Dubord, Bodovoahangy Andriatiana, and Priscille Hertault from the CAAST in the Alfort school of veterinary medicine for the biochemical analyses. We thank Pr Valérie Chetboul and Dr Vassiliki Gouni, as well as the cardiology unit team of the Alfort school of veterinary medicine for the echocardiographic measures. We thank all the adoptants of the healthy males and the retired carrier females for having offered them a second life in a family, and the association GRAAL for their help to the implementation of the "4th R". We thank Dr Pablo Aguilar, Xavier Cauchois and all the animal keepers who have taken care of our friendly and sweet LRMD companions over the past years.

References

1. Mah JK, Korngut L, Dykeman J, Day L, Pringsheim T, Jette N. A systematic review and meta-analysis on the epidemiology of Duchenne and Becker muscular dystrophy. Neuromuscul.Disord. 2014;24:482-491
2. Bushby K, Finkel R, Birnkrant DJ, Case LE, Clemens PR, Cripe L, et al. Diagnosis and management of Duchenne muscular dystrophy, part 1: diagnosis, and pharmacological and psychosocial management. Lancet Neurol. 2010;9:77-93
3. Passamano L, Taglia A, Palladino A, Viggiano E, D'Ambrosio P, Scutifero M, et al. Improvement of survival in Duchenne Muscular Dystrophy: retrospective analysis of 835 patients. Acta Myol. 2012;31:121-125
4. Valentine BA, Cooper BJ, de LA, O'Quinn R, Blue JT. Canine X-linked muscular dystrophy. An animal model of Duchenne muscular dystrophy: clinical studies. J.Neurol.Sci. 1988;88:69-81

5. Kornegay JN, Bogan JR, Bogan DJ, Childers MK, Li J, Nghiem P, et al. Canine models of Duchenne muscular dystrophy and their use in therapeutic strategies. Mamm.Genome 2012;23:85-108
6. Duan D. Duchenne muscular dystrophy gene therapy: Lost in translation? Res.Rep.Biol. 2011;2011:31-42
7. Banks GB, Chamberlain JS. The value of mammalian models for duchenne muscular dystrophy in developing therapeutic strategies. Curr.Top.Dev.Biol. 2008;84:431-453
8. Wentink GH, Van Der Linde-Sipman JS, Meijer AEFH, Kamphuisen HAC, Van Vorstenbosch CJAHV, Hartman W, et al. Myopathy with a Possible Recessive X-linked Inheritance in a Litter of Irish Terriers. Vet.Pathol. 1972;9:328-349
9. Kornegay JN, Tuler SM, Miller DM, Levesque DC. Muscular dystrophy in a litter of golden retriever dogs. Muscle Nerve 1988;11:1056-1064
10. Gorospe J, Hoffman E, McQuarrie P, Cardinet G. Duchenne muscular dystrophy in a wire-haired fox (WHF) terrier: a new dog model with no somatic reversion. Proceedings of the VIIIth Congress on Human Genetics 1991;97
11. Paola JP, Podell M, Shelton GD. Muscular Dystrophy in a Miniature Schnauzer. Progress in Veterinary Neurology 1993;4:14-18
12. Presthus J, Nordstoga K. Congenital Myopathy in a Litter of Samoyed Dogs. Progress in Veterinary Neurology 1993;4:37-40
13. Van Ham LML, Desmidt M, Tshamala M, Hoorens JK, Mattheeuws DRG. Canine X-linked Muscular Dystrophy in Belgian Groenendaeler Shepherds. J.Am.Anim Hosp.Assoc. 1993;29:570-574
14. Winand N, Pradham D, Cooper B. Molecular characterization of severe Duchenne-tupe muscular dystrophy in a family of Rottweiler dogs. Molecular Mechanism of Neuromuscular Disease.Muscular Dystrophy Association, Tucson (AZ), USA. 1994;
15. Van Ham LML, Roels SLMF, Hoorens JK. Congenital Dystrophy-like Myopathy in a Brittany Spaniel Puppy. Progress in Veterinary Neurology 1995;6:135-138
16. Schatzberg SJ, Olby NJ, Breen M, Anderson LV, Langford CF, Dickens HF, et al. Molecular analysis of a spontaneous dystrophin 'knockout' dog. Neuromuscul.Disord. 1999;9:289-295
17. Wetterman CA, Harkin KR, Cash WC, Nietfield JC, Shelton GD. Hypertrophic Muscular Dystrophy in a Young Dog. JAVMA 2000;216:878-881
18. Bergman RL, Inzana KD, Monroe WE, Shell LG, Liu LA, Engvall E, et al. Dystrophin-deficient muscular dystrophy in a Labrador retriever. J.Am.Anim Hosp.Assoc. 2002;38:255-261
19. Wieczorek LA, Garosi LS, Shelton GD. Dystrophin-deficient muscular dystrophy in an old English sheepdog. Vet.Rec. 2006;158:270-273
20. Baltzer WI, Calise DV, Levine JM, Shelton GD, Edwards JF, Steiner JM. Dystrophin-deficient muscular dystrophy in a Weimaraner. J.Am.Anim Hosp.Assoc. 2007;43:227-232
21. Klarenbeek S, Gerritzen-Bruning MJ, Rozemuller AJ, van der Lugt JJ. Canine X-linked muscular dystrophy in a family of Grand Basset Griffon Vendeen dogs. J.Comp Pathol. 2007;137:249-252

22. Smith BF, Yue Y, Woods PR, Kornegay JN, Shin JH, Williams RR, et al. An intronic LINE-1 element insertion in the dystrophin gene aborts dystrophin expression and results in Duchenne-like muscular dystrophy in the corgi breed. Lab Invest 2010;
23. Walmsley GL, rechavala-Gomeza V, Fernandez-Fuente M, Burke MM, Nagel N, Holder A, et al. A duchenne muscular dystrophy gene hot spot mutation in dystrophin-deficient cavalier king charles spaniels is amenable to exon 51 skipping. PLoS.One. 2010;5:e8647
24. Ito D, Kitagawa M, Jeffery N, Okada M, Yoshida M, Kobayashi M, et al. Dystrophin-deficient muscular dystrophy in an Alaskan malamute. Vet.Rec. 2011;169:127
25. Baroncelli AB, Abellonio F, Pagano TB, Esposito I, Peirone B, Papparella S, et al. Muscular dystrophy in a dog resembling human becker muscular dystrophy. J.Comp Pathol. 2014;150:429-433
26. Vieira NM, Guo LT, Estrela E, Kunkel LM, Zatz M, Shelton GD. Muscular dystrophy in a family of Labrador Retrievers with no muscle dystrophin and a mild phenotype. Neuromuscul.Disord. 2015;25:363-370
27. Jenkins CA, Forman OP. Identification of a novel frameshift mutation in the DMD gene as the cause of muscular dystrophy in a Norfolk terrier dog. Canine.Genet.Epidemiol. 2015;2:7
28. Giannasi C, Tappin SW, Guo LT, Shelton GD, Palus V. Dystrophin-deficient muscular dystrophy in two lurcher siblings. J.Small Anim Pract. 2015;56:577-580
29. Atencia-Fernandez S, Shiel RE, Mooney CT, Nolan CM. Muscular dystrophy in the Japanese Spitz: an inversion disrupts the DMD and RPGR genes. Anim Genet. 2015;46:175-184
30. Nghiem PP, Bello L, Balog-Alvarez C, Lopez SM, Bettis A, Barnett H, et al. Whole genome sequencing reveals a 7 base-pair deletion in DMD exon 42 in a dog with muscular dystrophy. Mamm.Genome 2017;28:106-113
31. Sanchez L, Beltran E, de SA, Guo LT, Shea A, Shelton GD, et al. Clinical and genetic characterisation of dystrophin-deficient muscular dystrophy in a family of Miniature Poodle dogs. PLoS.One. 2018;13:e0193372
32. Mata LS, Hammond JJ, Rigsby MB, Balog-Alvarez CJ, Kornegay JN, Nghiem PP. A novel canine model for Duchenne muscular dystrophy (DMD): single nucleotide deletion in DMD gene exon 20. Skelet.Muscle 2018;8:16
33. Shrader SM, Jung S, Denney TS, Smith BF. Characterization of Australian Labradoodle dystrophinopathy. Neuromuscul.Disord. 2018;
34. Jeandel A, Garosi LS, Davies L, Guo LT, Salguero R, Shelton GD. Late-onset Becker-type muscular dystrophy in a Border terrier dog. J.Small Anim Pract. 2018;
35. VanBelzen DJ, Malik AS, Henthorn PS, Kornegay JN, Stedman HH. Mechanism of Deletion Removing All Dystrophin Exons in a Canine Model for DMD Implicates Concerted Evolution of X Chromosome Pseudogenes. Mol.Ther.Methods Clin.Dev. 2017;4:62-71
36. Sharp NJ, Kornegay JN, Van Camp SD, Herbstreith MH, Secore SL, Kettle S, et al. An error in dystrophin mRNA processing in golden retriever muscular dystrophy, an animal homologue of Duchenne muscular dystrophy. Genomics 1992;13:115-121

37. Shimatsu Y, Katagiri K, Furuta T, Nakura M, Tanioka Y, Yuasa K, et al. Canine X-linked muscular dystrophy in Japan (CXMDJ). Exp.Anim 2003;52:93-97
38. Barthelemy I, Pinto-Mariz F, Yada E, Desquilbet L, Savino W, Silva-Barbosa SD, et al. Predictive markers of clinical outcome in the GRMD dog model of Duchenne muscular dystrophy. Dis.Model.Mech. 2014;7:1253-1261
39. Vieira NM, Elvers I, Alexander MS, Moreira YB, Eran A, Gomes JP, et al. Jagged 1 Rescues the Duchenne Muscular Dystrophy Phenotype. Cell 2015;163:1204-1213
40. Vieira NM, Spinazzola JM, Alexander MS, Moreira YB, Kawahara G, Gibbs DE, et al. Repression of phosphatidylinositol transfer protein alpha ameliorates the pathology of Duchenne muscular dystrophy. Proc.Natl.Acad.Sci.U.S.A 2017;114:6080-6085
41. Vulin A, Barthelemy I, Goyenvalle A, Thibaud JL, Beley C, Griffith G, et al. Muscle Function Recovery in Golden Retriever Muscular Dystrophy After AAV1-U7 Exon Skipping. Mol.Ther. 2012;20:2120-2133
42. Sampaolesi M, Blot S, D'Antona G, Granger N, Tonlorenzi R, Innocenzi A, et al. Mesoangioblast stem cells ameliorate muscle function in dystrophic dogs. Nature 2006;444:574-579
43. Hammers DW, Sleeper MM, Forbes SC, Coker CC, Jirousek MR, Zimmer M, et al. Disease-modifying effects of orally bioavailable NF-kappaB inhibitors in dystrophin-deficient muscle. JCI.Insight. 2016;1:e90341
44. Le GC, Servais L, Montus M, Larcher T, Fraysse B, Moullec S, et al. Long-term microdystrophin gene therapy is effective in a canine model of Duchenne muscular dystrophy. Nat.Commun. 2017;8:16105
45. Willmann R, Possekel S, Dubach-Powell J, Meier T, Ruegg MA. Mammalian animal models for Duchenne muscular dystrophy. Neuromuscul.Disord. 2009;19:241-249
46. Amoasii L, Hildyard JCW, Li H, Sanchez-Ortiz E, Mireault A, Caballero D, et al. Gene editing restores dystrophin expression in a canine model of Duchenne muscular dystrophy. Science 2018;362:86-91
47. Thibaud JL, Monnet A, Bertoldi D, Barthelemy I, Blot S, Carlier PG. Characterization of dystrophic muscle in golden retriever muscular dystrophy dogs by nuclear magnetic resonance imaging. Neuromuscul.Disord. 2007;17:575-584
48. Barthelemy I, Barrey E, Thibaud JL, Uriarte A, Voit T, Blot S, et al. Gait analysis using accelerometry in dystrophin-deficient dogs. Neuromuscul.Disord. 2009;19:788-796
49. Barthelemy I, Barrey E, Aguilar P, Uriarte A, Le CM, Thibaud JL, et al. Longitudinal ambulatory measurements of gait abnormality in dystrophin-deficient dogs. BMC.Musculoskelet.Disord. 2011;12:75
50. Barthelemy I, Uriarte A, Drougard C, Unterfinger Y, Thibaud JL, Blot S. Effects of an Immunosuppressive Treatment in the GRMD Dog Model of Duchenne Muscular Dystrophy. PLoS.One. 2012;7:e48478
51. Barthelemy I, Thibaud JL, Vulin A, Bertoldi D, Goyenvalle A, Lorain S, et al. Functional evaluation of dystrophic dogs treated by exon-skipping. Neuromuscul.Disord. 2007;17:898

52. DeVanna JC, Kornegay JN, Bogan DJ, Bogan JR, Dow JL, Hawkins EC. Respiratory dysfunction in unsedated dogs with golden retriever muscular dystrophy. Neuromuscul.Disord. 2014;24:63-73
53. Chetboul V, Escriou C, Tessier D, Richard V, Pouchelon JL, Thibault H, et al. Tissue Doppler imaging detects early asymptomatic myocardial abnormalities in a dog model of Duchenne's cardiomyopathy. Eur.Heart J. 2004;25:1934-1939
54. Adiconis X, Borges-Rivera D, Satija R, DeLuca DS, Busby MA, Berlin AM, et al. Comparative analysis of RNA sequencing methods for degraded or low-input samples. Nat.Methods 2013;10:623-629
55. Bolger AM, Lohse M, Usadel B. Trimmomatic: a flexible trimmer for Illumina sequence data. Bioinformatics. 2014;30:2114-2120
56. Dobin A, Davis CA, Schlesinger F, Drenkow J, Zaleski C, Jha S, et al. STAR: ultrafast universal RNA-seq aligner. Bioinformatics. 2013;29:15-21
57. Nguyen F, Cherel Y, Guigand L, Goubault-Leroux I, Wyers M. Muscle lesions associated with dystrophin deficiency in neonatal golden retriever puppies. J.Comp Pathol. 2002;126:100-108
58. Bedu AS, Labruyere JJ, Thibaud JL, Barthelemy I, Leperlier D, Saunders JH, et al. Age-related thoracic radiographic changes in golden and labrador retriever muscular dystrophy. Vet.Radiol.Ultrasound 2012;53:492-500
59. Flanigan KM, Ceco E, Lamar KM, Kaminoh Y, Dunn DM, Mendell JR, et al. LTBP4 genotype predicts age of ambulatory loss in duchenne muscular dystrophy. Ann.Neurol. 2012;
60. Heydemann A, Ceco E, Lim JE, Hadhazy M, Ryder P, Moran JL, et al. Latent TGF-beta-binding protein 4 modifies muscular dystrophy in mice. J.Clin.Invest 2009;119:3703-3712
61. Bladen CL, Salgado D, Monges S, Foncuberta ME, Kekou K, Kosma K, et al. The TREAT-NMD DMD Global Database: analysis of more than 7,000 Duchenne muscular dystrophy mutations. Hum.Mutat. 2015;36:395-402
62. Vulin A, Wein N, Simmons TR, Rutherford AM, Findlay AR, Yurkoski JA, et al. The first exon duplication mouse model of Duchenne muscular dystrophy: A tool for therapeutic development. Neuromuscul.Disord. 2015;25:827-834
63. Aartsma-Rus A, van Deutekom JC, Fokkema IF, Van Ommen GJ, den Dunnen JT. Entries in the Leiden Duchenne muscular dystrophy mutation database: an overview of mutation types and paradoxical cases that confirm the reading-frame rule. Muscle Nerve 2006;34:135-144
64. Konagaya M, Honda H, Sakai M, Iida M. Transmission of dystrophinopathy by X-chromosome inversion. Neurology 1995;45:1409-1410
65. Shashi V, Golden WL, Allinson PS, Blanton SH, von Kap-Herr C, Kelly TE. Molecular analysis of recombination in a family with Duchenne muscular dystrophy and a large pericentric X chromosome inversion. Am.J.Hum.Genet. 1996;58:1231-1238
66. Baxter PS, Maltby EL, Quarrell O. Xp21 muscular dystrophy due to X chromosome inversion. Neurology 1997;49:260

67. Bhat SS, Schmidt KR, Ladd S, Kim KC, Schwartz CE, Simensen RJ, et al. Disruption of DMD and deletion of ACSL4 causing developmental delay, hypotonia, and multiple congenital anomalies. Cytogenet.Genome Res. 2006;112:170-175
68. Tran TH, Zhang Z, Yagi M, Lee T, Awano H, Nishida A, et al. Molecular characterization of an X(p21.2;q28) chromosomal inversion in a Duchenne muscular dystrophy patient with mental retardation reveals a novel long non-coding gene on Xq28. J.Hum.Genet. 2013;58:33-39
69. Schatzberg SJ, Anderson LV, Wilton SD, Kornegay JN, Mann CJ, Solomon GG, et al. Alternative dystrophin gene transcripts in golden retriever muscular dystrophy. Muscle Nerve 1998;21:991-998
70. Christophe-Hobertus C, Szpirer C, Guyon R, Christophe D. Identification of the gene encoding Brain Cell Membrane Protein 1 (BCMP1), a putative four-transmembrane protein distantly related to the Peripheral Myelin Protein 22 / Epithelial Membrane Proteins and the Claudins. BMC.Genomics 2001;2:3
71. Utami KH, Hillmer AM, Aksoy I, Chew EG, Teo AS, Zhang Z, et al. Detection of chromosomal breakpoints in patients with developmental delay and speech disorders. PLoS.One. 2014;9:e90852
72. Christophe-Hobertus C, Kooy F, Gecz J, Abramowicz MJ, Holinski-Feder E, Schwartz C, et al. TM4SF10 gene sequencing in XLMR patients identifies common polymorphisms but no disease-associated mutation. BMC.Med.Genet. 2004;5:22
73. Gonorazky H, Liang M, Cummings B, Lek M, Micallef J, Hawkins C, et al. RNAseq analysis for the diagnosis of muscular dystrophy. Ann.Clin.Transl.Neurol. 2016;3:55-60
74. Cummings BB, Marshall JL, Tukiainen T, Lek M, Donkervoort S, Foley AR, et al. Improving genetic diagnosis in Mendelian disease with transcriptome sequencing. Sci.Transl.Med. 2017;9:
75. de Leon MB, Montanez C, Gomez P, Morales-Lazaro SL, Tapia-Ramirez V, Valadez-Graham V, et al. Dystrophin Dp71 expression is down-regulated during myogenesis: role of Sp1 and Sp3 on the Dp71 promoter activity. J.Biol.Chem. 2005;280:5290-5299
76. Chamberlain JS, Corrado K, Rafael JA, Cox GA, Hauser M, Lumeng C. Interactions between dystrophin and the sarcolemma membrane. Soc.Gen.Physiol Ser. 1997;52:19-29
77. Wieneke S, Heimann P, Leibovitz S, Nudel U, Jockusch H. Acute pathophysiological effects of muscle-expressed Dp71 transgene on normal and dystrophic mouse muscle. J.Appl.Physiol (1985.) 2003;95:1861-1866
78. Greenberg DS, Sunada Y, Campbell KP, Yaffe D, Nudel U. Exogenous Dp71 restores the levels of dystrophin associated proteins but does not alleviate muscle damage in mdx mice. Nat.Genet. 1994;8:340-344

Figures

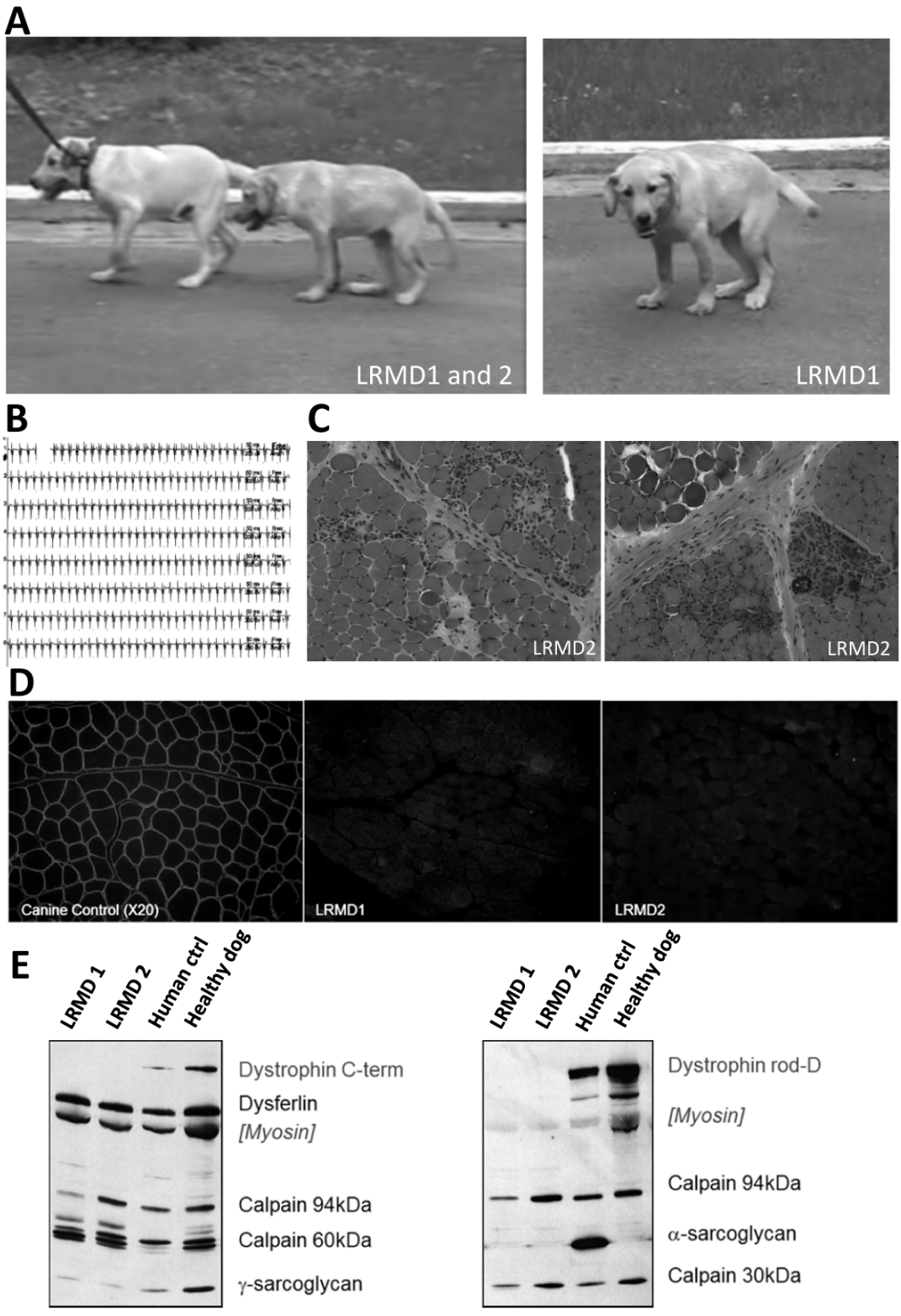

Figure 1

First cases' findings orientate towards a dystrophinopathy. A: Pictures of the two first affected brothers (LRMD1 and 2), at 4 months of age, at time of their presentation to the neurology consultation of the Alfort school of veterinary medicine. Note the markedly plantigradic and palmigradic posture and the pelvic verticalization. B: Electromyographic recording showing complex repetitive discharges, observed in both animals especially in proximal appendicular muscles. C: H&E stainings of a biceps femoris biopsy

taken from LRMD2 at 4 months of age, showing a dystrophic profile: necrosis, regeneration, endomysial fibrosis, hypercontracted fibers, inflammatory foci and calcifications. D: Dystrophin (rod-domain) immunostaining in LRMD1 and 2 biceps femoris muscles compared to an unaffected dog, showing the absence of signal delineating the membrane of the muscle fibers, as it is seen in the control dog. E: Multiplex western-blot confirming the absence of dystrophin immunoreactivity in the two affected dogs, using two different anti-dystrophin antibodies (Dys2, anti- C-terminal part, and Dys1, anti- rod domain). The γ-sarcoglycan was present in both affected dogs however weaker than in the healthy dog, probably because of a disruption of the dystrophin-associated protein complex. The other revealed proteins were unmodified, except the α-sarcoglycan for which the human antibody showed no cross-reactivity with canine muscles.

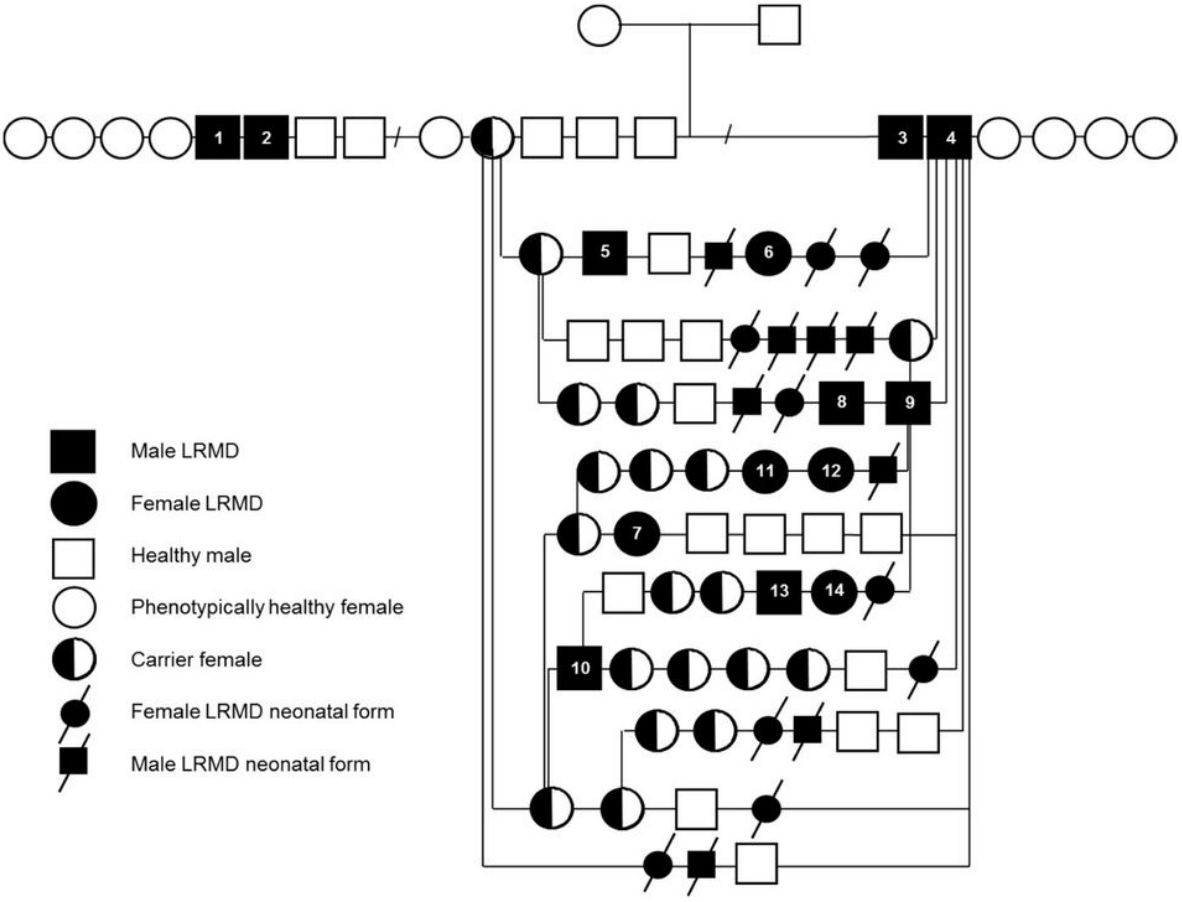

Figure 2

Pedigree of the LRMD colony. The colony was founded using a crossing between an affected male and his carrier sister. Ten subsequent litters were obtained, and a total of 14 LRMD dogs could be examined exception made of the deceased neonate puppies. A high inbreeding level was present in the colony (consanguinity coefficients min 25 % max 41 %).

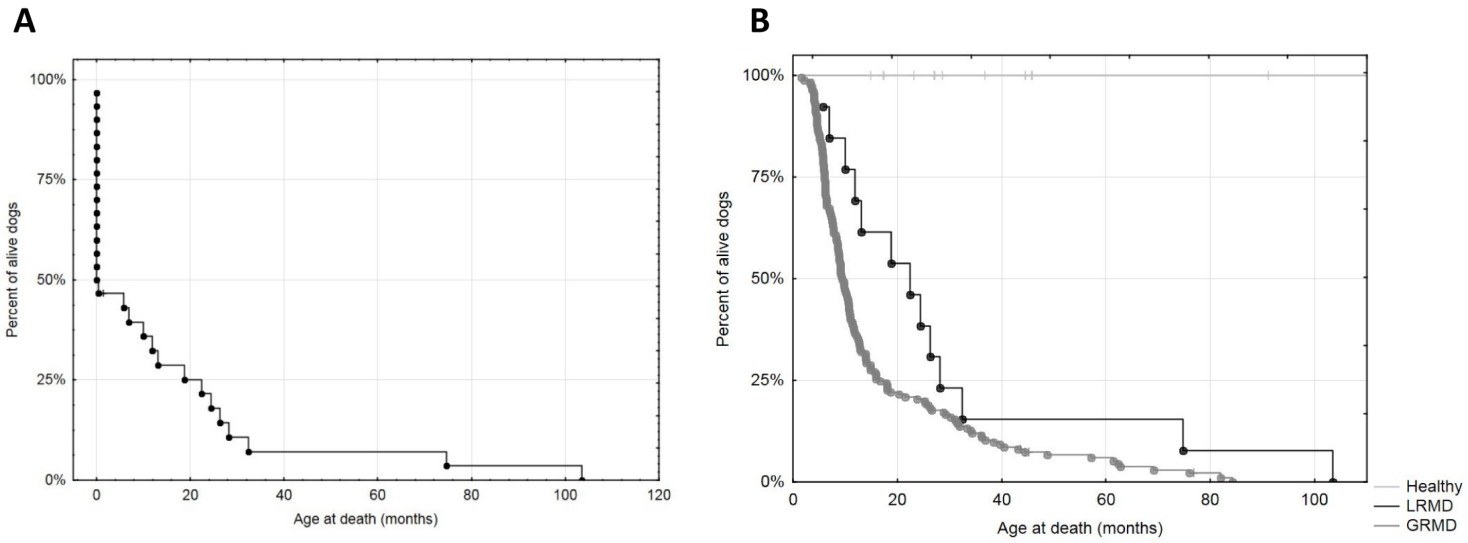

Figure 3

Survival of LRMD dogs. A: Kaplan-Meier survival curve showing that half of the LRMD dogs die within their first days of life due to neonatal fulminating forms, only 25 % of the LRMD dogs survived more than 18.9 months. The longest survival was 103.5 months in one LRMD dog. B: Kaplan-Meier survival curve comparing LRMD to GRMD and healthy dogs' survival without taking into account the neonatal period (beginning of the follow-up: 2 months of age). In both colonies the survival was markedly impaired compared with healthy dogs. However the LRMD survival seemed better, and this trend was confirmed by a significant log rank test (p = 0.01).

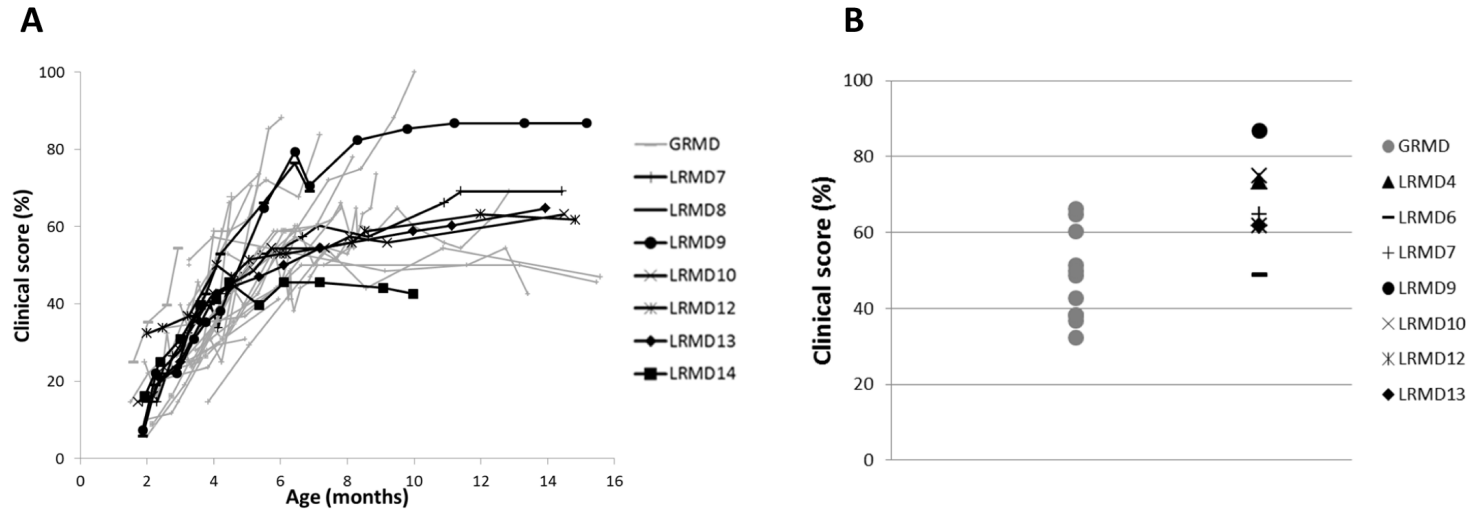

Figure 4

Clinical scoring in LRMD dogs. GRMD dogs are represented in gray, and LRMD dogs in black. A: longitudinal evolution of the clinical score during the progressive phase of the disease. In both colonies, the clinical score is low at the age of two months and rapidly increases to roughly stabilize after the age of 8 months, signing the rapid aggravation of the clinical signs in the first months. Although apparently

more homogeneous during the 2-4 months period with a rapid evolution in all the studied dogs, the clinical scores of LRMD dogs became more heterogeneous afterwards, with two dogs presenting with a more severe evolution, and one with a milder. This shows that a phenotypic heterogeneity is present in this colony as well as in GRMD dogs in which it is well-known. At later stages the clinical scores of LRMD dogs seemed more elevated than those obtained in GRMD dogs. This was confirmed by a comparison in adult dogs: B: comparison of clinical scores in adult LRMD vs GRMD dogs. The clinical scores obtained in adult clinically stabilized LRMD dogs were significantly increased in comparison to GRMD dogs ($p = 0.005$), suggesting that adult LRMD dogs could be globally more affected than GRMD dogs. However the values of both colonies were partly overlapping.

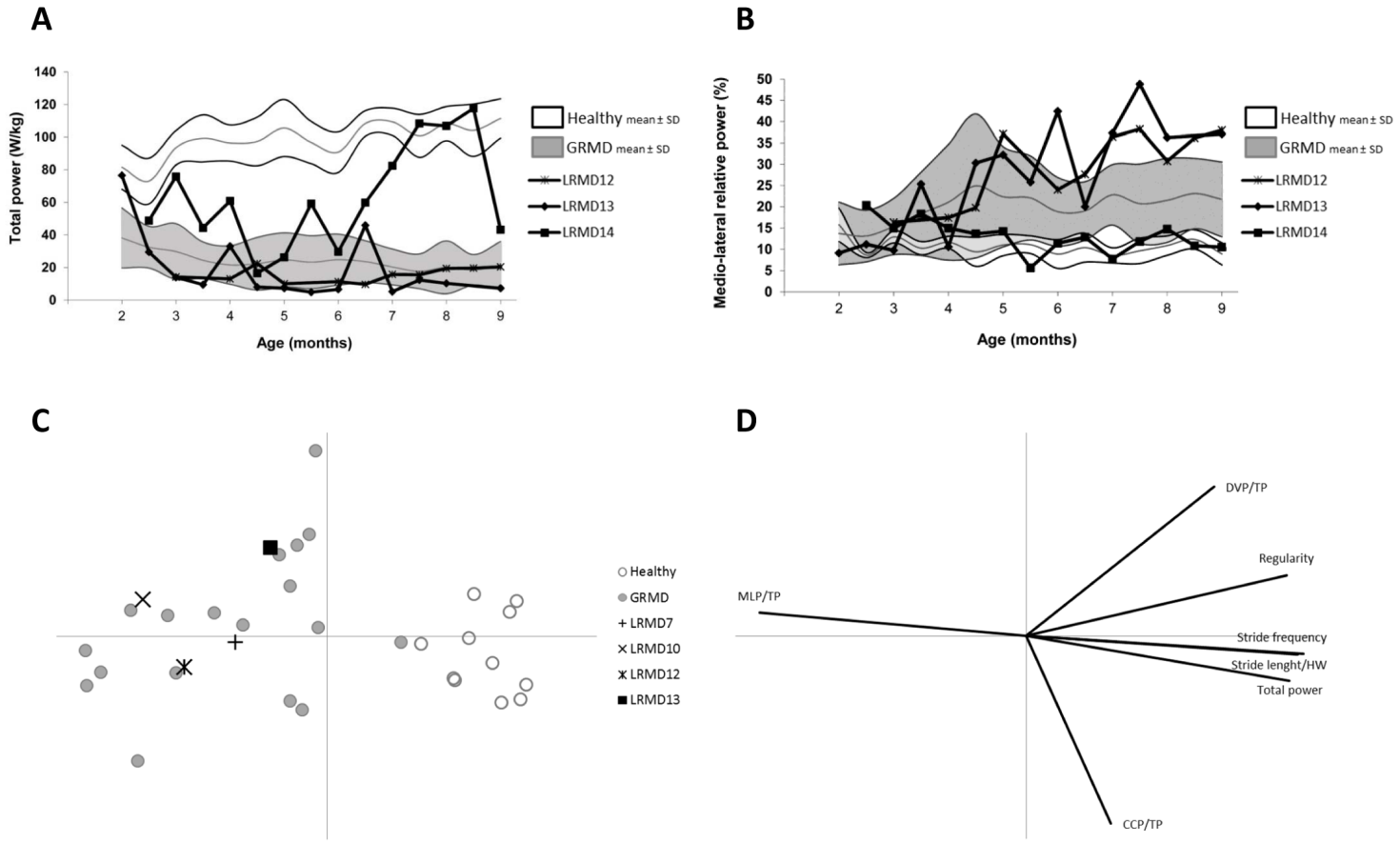

Figure 5

Gait analysis in LRMD dogs using accelerometry. A and B: longitudinal follow-up in 3 LRMD dogs during the evolutive phase of the disease. The white and gray areas respectively represent the mean ± 1 SD of the healthy dogs and GRMD dogs populations; the black curves represent the evolution of each of the three LRMD dogs. A: evolution of the total power from the age of 2 to the age of 9 months. Two among the three LRMD dogs had markedly decreased total power values, at levels comparable to GRMD dogs. The third one (LRMD14) exhibited rather preserved total power values, especially in the second part of the follow-up, from the age of 6.5 months, where some values overlapped with healthy dogs ones. B: evolution of the relative medio-lateral power from the age of 2 to the age of 9 months. Two among the three LRMD dogs showed a dramatic increase of their medio-lateral relative power with age and disease

progression, while the third dog (LRMD14) maintained normal values all along the follow-up period. C: projection of 4 adult LRMD dogs as supplementary individuals on a PCA (principal component analysis) plane built with adult healthy and GRMD dogs as active individuals. Healthy and GRMD populations are well separated and LRMD dogs appear in the cloud of GRMD dogs. D: projection of the variables. The dispersion of the dystrophic populations from the healthy one is mainly explained by decreased total power, stride length and frequency, and increased medio-lateral power. Abbreviations: MLP/TP: medio-lateral power/total power; DVP/TP: dorso-ventral power/total power; CCP/TP: cranio-caudal power/total power; HW: height at withers.

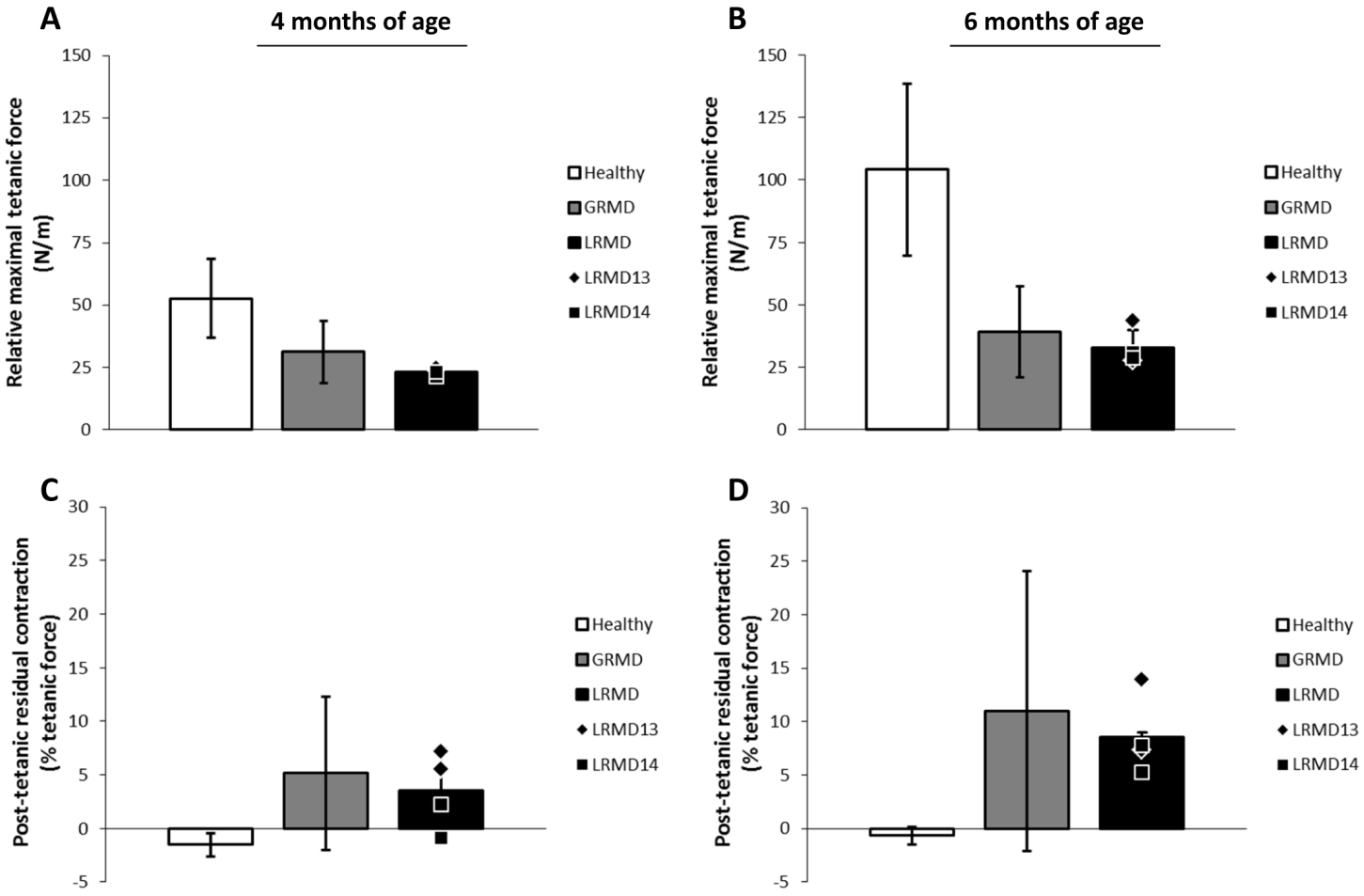

Figure 6

Force and relaxation measurement in LRMD dogs at 4 and 6 months of age. The histograms represent the mean value of the healthy (white), GRMD (gray) or LRMD (black) populations, and the error bars ±1 SD. The black symbols represent the individual values of the two LRMD dogs studied (2 legs measured each). A and B: relative maximal tetanic force, at 4 (A) and 6 (B) months of age, obtained after a normalization by the leg length in order to take into account differences in dogs' size. The muscle force appeared decreased in LRMD dogs, at a slightly lower level than GRMD dogs at 4 months and 6 months. C and D: post-tetanic residual contraction as a percentage of the tetanic force at 4 (C) and 6 (D) months of age, was measured by normalizing the difference between pre- and post-tetanic baselines by the

maximal tetanic force. An incomplete relaxation after a tetanic stimulation was observed in LRMD dogs as in GRMD dogs, with an increase of this relaxation defect with age.

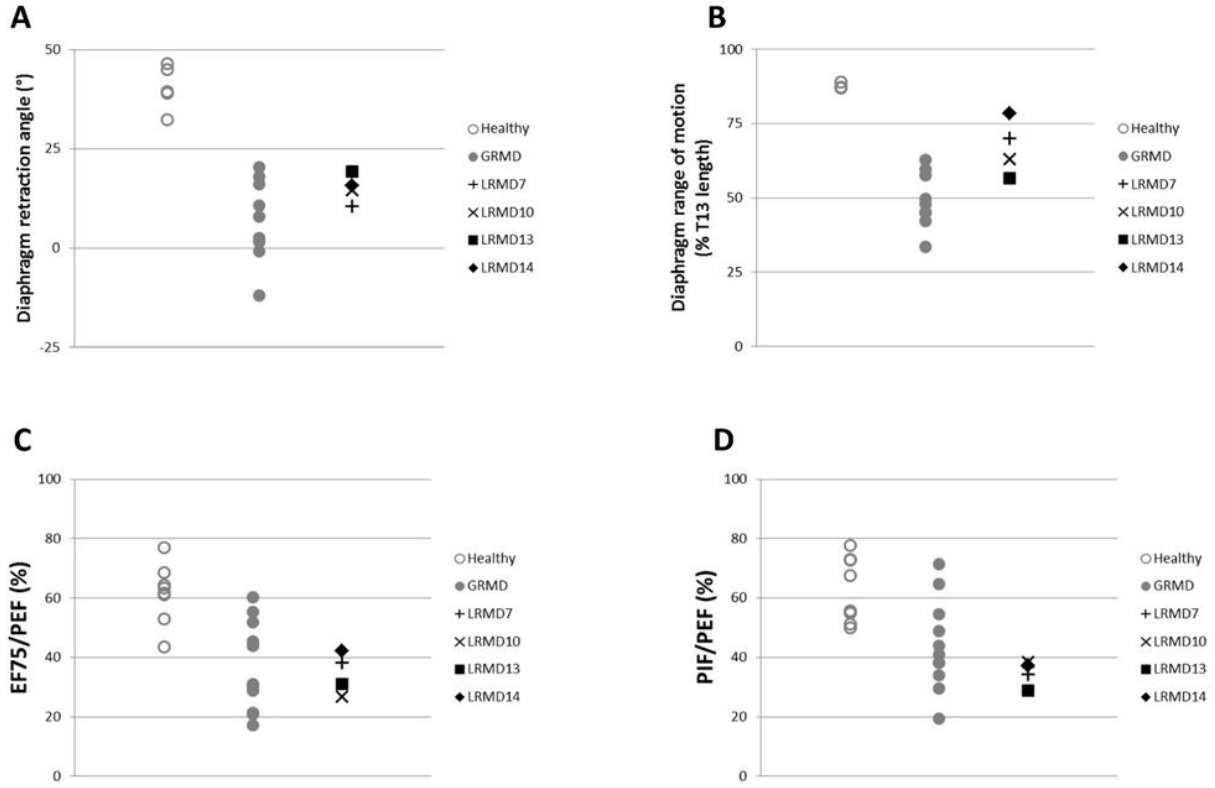

Figure 7

Respiratory function in LRMD dogs. Healthy dogs are represented by empty gray circles, GRMD dogs by gray dots, and LRMD dogs by black symbols. All the dogs were adults (>10 months). A and B: results of diaphragmatic kinematics on videofluoroscopic acquisitions. A: The angle formed at the ventral diaphragmatic edge of the caudal vena cava foramen, by a perpendicular to the vertebral axis and a straight line joining the caudal edge of the 11th thoracic vertebra is reduced in LRMD dogs attesting to the caudal retraction of the diaphragm at similar levels as GRMD dogs. B : The diaphragm range of motion is decreased in LRMD dogs compared to healthy dogs, but to a lesser extent than GRMD dogs. C and D : results from spirometric acquisitions. C: the expiratory flow at 75 % of the expired volume, expressed as a percentage of the peak expiratory flow, is decreased in LRMD dogs, in comparison to healthy dogs, with values overlapping those obtained in GRMD dogs. D: The ratio of the peak inspiratory flow on the peak expiratory flow is decreased in LRMD dogs, overlapping the lowest values obtained in the GRMD population. Abbreviations: T13: 13th thoracic vertebra; EF75: expiratory flow at 75 % of the expired volume; PEF: peak expiratory flow; PIF: peak inspiratory flow.

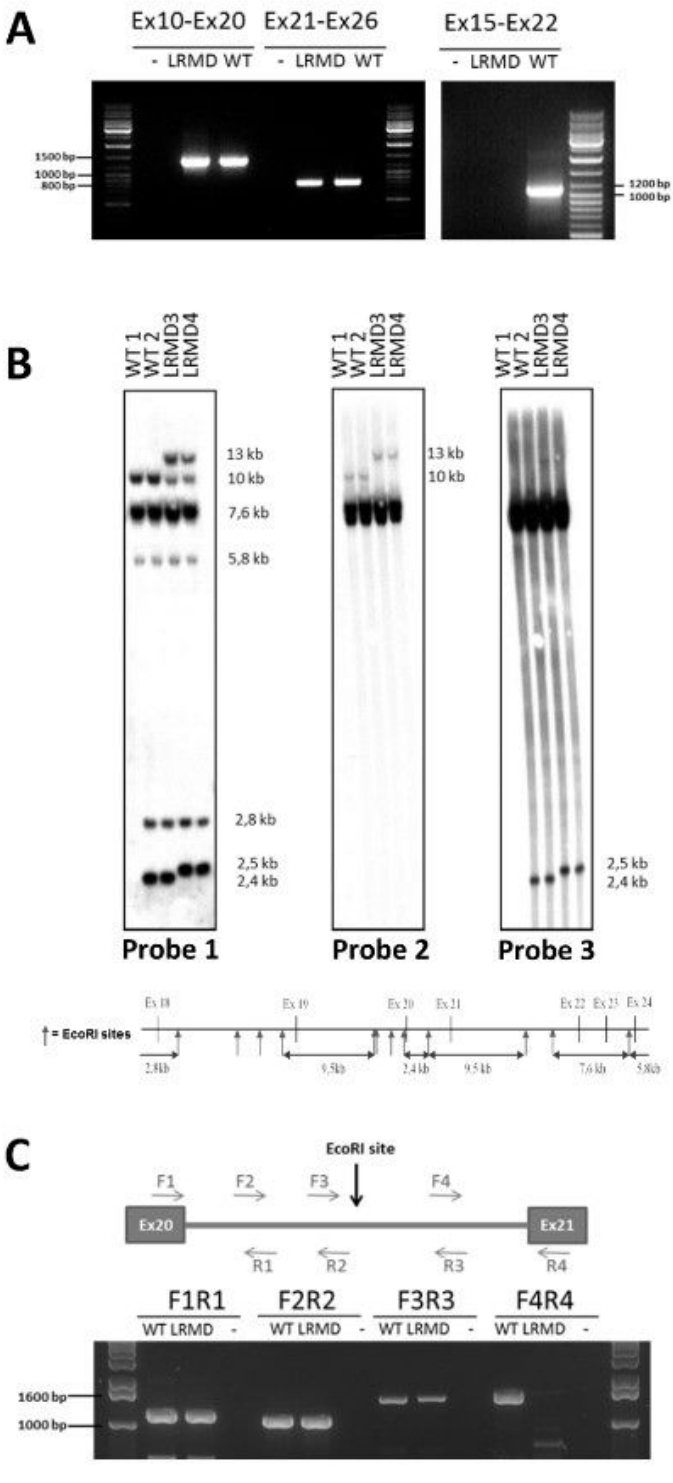

Figure 8

Mapping of the LRMD mutation. A: Nested RT-PCR on the DMD cDNA. Normal-sized amplicons were obtained in LRMD dogs all along the cDNA, including using primers in exons 10 and 20 (expected size 1373 bp) or exons 21 and 26 (expected size 807 bp). A RT-PCR using primers in exons 15 and 22 yields a normal-sized amplicons (1095 bp) in the WT dog, but no band in the LRMD dog. B: Southern blot on the gDNA from two WT Labrador dogs unrelated to the LRMD colony, and two LRMD dogs after an EcoRI

digestion. The EcoRI restriction map of this region is schematized below the southern blot. The digestion profile revealed by Probe 1 covering exons 18-24 differs from the WT in the two LRMD dogs, with an extra-band around 13 kb and a 2.5 kb band replacing the 2.4 kb wild-type band. The use of Probe 2 covering exon 21 shows an abnormal band at 13 kb, shifted from its normal size at 10 kb is in the restriction fragment containing the exon 21, which normal size is 10 kb. The use of Probe 3 covering exon 20 shows an abnormal band at 2.5 kb, shifted from its normal size at 2.4 kb. These results suggest a gross rearrangement in the intron 20. C: Exploration of intron 20 (4.5 kb in WT dogs) by PCR, using 4 overlapping reactions, in a LRMD vs a WT littermate, showing that a band at normal size could be obtained using the first three pairs of primers. The last pair exploring a 1661 bp zone including the junction between intron 20 and exon 21, downstream the EcoRI site, failed to amplify any product in LRMD dogs, even using long-range PCR conditions.

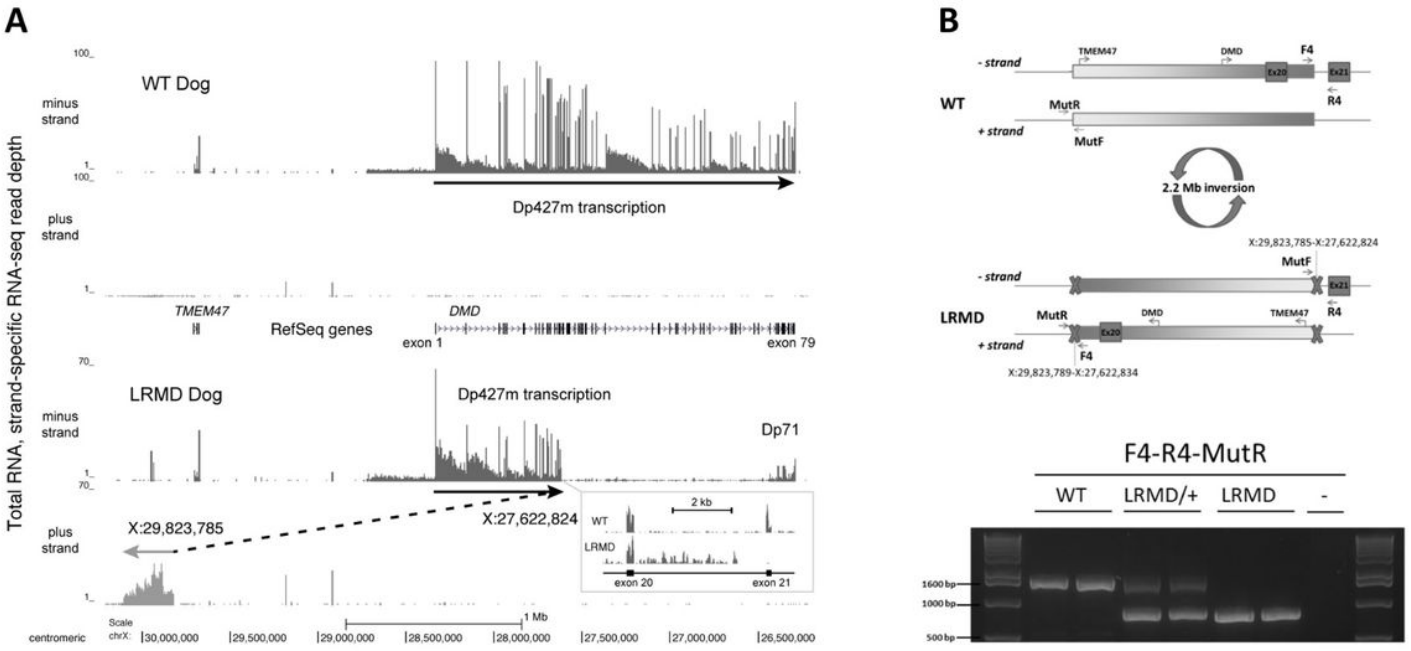

Figure 9

RNA-seq-based identification of the LRMD mutation. A: A 4 Mb region spanning canFam3 chrX:30,200,000-26,200,000 is shown with RNA-seq read depths observed in biceps femoris biopsy experiment plotted with RefSeq gene annotations. The upper panel shows the major Dp427m minus-strand transcript levels (DMD exons 1 through 79) seen with an unaffected dog, while the lower panel shows the inversion inferred from minus-strand DMD transcription and plus-strand ectopic transcription seen with LRMD8. The boxed inset shows a detailed view of intron 20 transcription from these two animals. B: Schematic representation of the LRMD mutation, and LRMD genetic diagnosis by PCR. Two pairs of primers were used: the first one F4-R4 amplifies a 1661 bp product in the WT dog but not in the LRMD dog (breakpoint between these two primers). A second pair of primers (MutF –MutR) was designed in the distant site across the breakpoint, allowing the amplification of a 1939 bp product in the WT situation but not in the LRMD (data not shown). The proposed diagnostic PCR test relies on the use

of F4 as a forward primer, and the combination of R4 and MutR as reverse primers to amplify the WT or the LRMD allele, respectively. Using this test, a unique PCR product around 1600 bp is observed in two LRMD healthy littermates (amplicon including F4-R4); a unique PCR product around 900 bp is observed in two affected LRMD dogs (amplicon including F4-mutR); and both amplicons are observed in carrier females.

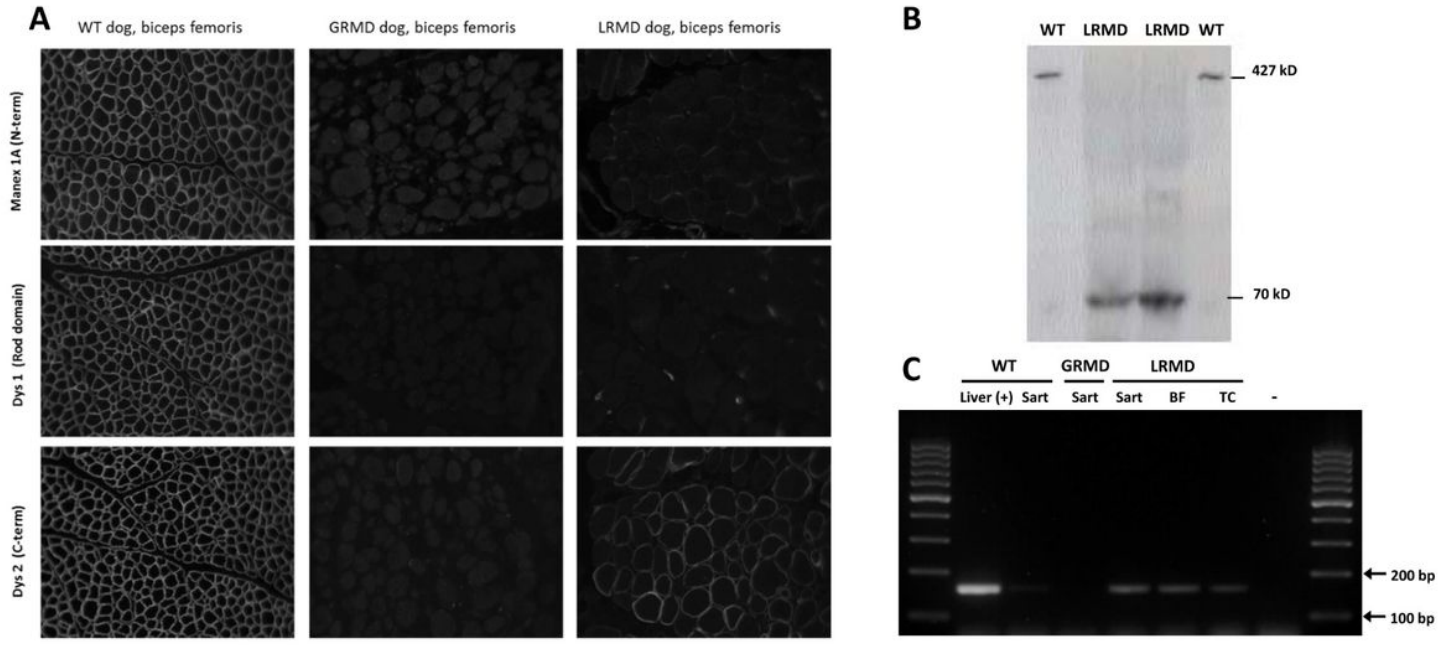

Figure 10

Expression of the Dp71 isoform in LRMD muscles. A: Comparative immunohistochemistry on biopsies from the biceps femoris muscle of a healthy dog, a GRMD dog and a LRMD dog. Three first antibodies were used: Manex 1A (N-terminal part), Dys 1 (Rod domain, downstream the mutation), Dys2 (C-terminal part). As expected, the staining was positive in the healthy dog, and negative for the GRMD dogs using the three antibodies. In the LRMD dog, the staining was negative with Manex 1A and Dys 1, and positive with Dys 2, with a heterogeneous level from one fiber to another. B: Western blotting using the Dys 2 antibody (C-terminal part). Muscle protein extracts from two healthy samples were loaded in wells 1 and 4 (50 µg) showing a band at the normal size of the full-length dystrophin (427 kD). Muscle protein extracts from LRMD muscles (250 µg) were loaded in wells 2 (LRMD3, biceps femoris) and 3 (LRMD3, interosseus muscle), showing a band at around 70 kD. C: RT-PCR using a forward primer designed at the junction between the specific first exon of the Dp71 and the exon 64, and a reverse primer at the junction between exons 65 and 66. cDNA from a canine liver was used as a positive control showing a band at expected size (164 bp). A very faint band was obtained using the cDNA from a healthy dog, and no band for the GRMD dog. Conversely, in the three cDNAs originating from LRMD muscles (LRMD 8, sartorius cranialis, biceps femoris, tibialis cranialis) a band at the same size as the positive control, though less strong, was seen, showing that the Dp71 transcript is present in LRMD muscles. Abbreviations: Sart: sartorius cranialis muscle; BF: biceps femoris muscle; TC: tibialis cranialis muscle.

Supplementary Files

This is a list of supplementary files associated with this preprint. Click to download.

- FigureS3.tif
- FigureS1.tif
- FigureS2.tif
- TableS2DMDdogmodelsv3.xlsx
- TableS1primers.docx